ABSTRACT

Title of Document:	Predicting thermally thin burning of polymer using TGA/DSC
	Mekyoung Kim, Master Thesis, 2006
Directed By:	James G. Quintiere**,** J.L. Bryan Professor, Department of Fire Protection Engineering

The flammability properties of pure Nylon 6 and Nylon with nano-clay of 5 % are examined in this study, TGA (Thermogravity Analysis) and DSC (Differential Scanning Calorimeter) data were obtained with a variety of heating rates. The decomposition rate was found from the analysis of TGA data based on the mass loss fraction. The rate of reaction was described by a first-order Arrhenius equation in terms of the active species and the char fraction. DSC yields the change of enthalpy of material as a function of temperature under the controlled temperature heating. The value of the temperature dependent specific heat capacity and heats of melting and decomposition of the materials were determined. With the kinetic and thermodynamic properties from TGA/DSC, the burning rate of thin polymers under radiant heat was formulated. The model results will be in terms of the derived TGA/DSC kinetic and thermodynamic properties compared to the data from the cone calorimeter experiments conducted by Xin Liu[1].

PREDICTING THERMALLY THIN BURNING OF POLYMER USING TGA/DSC

By

Mekyoung Kim

Thesis submitted to the Faculty of the Graduate School of the
University of Maryland, College Park, in partial fulfillment
of the requirements for the degree of
Master of Science
[2006]

Advisory Committee:
Professor James G. Quintiere, Chair
Professor James A. Milke
Professor Peter B. Sunderland

Acknowledgements

There have been a number of people without whom this thesis could not have been completed. My deepest gratitude goes to Dr. James G. Quintiere. He has tolerated an incalculable number of things from me. He has consistently helped me with great kindness and patience. Most of all, he showed me a model of what a life should be like. I also would like to thank my committee members: Dr. James A. Milke and Dr. Peter Sunderland for your support and time.

Research for this paper was supported in part by funds provided by the FAA. The FAA staff, Stas, was instrumental in providing a rigorous DSC method based on their calibration strategy. I have benefited greatly from that collaboration.

I have contracted many debt to my friends, Lian Danjun, Apinya, and Yunyong Utiskul who encouraging and full of useful suggestions.

I would like to express my undying gratitude to my family in Korea, for their love, care, physically and emotionally, and also Ankug E&C in Korea has supported me to pursuit this program here with all sorts of tangible and intangible stuffs.

Last but not least, I thank my God for great his love toward me. I can not help confessing this, everything comes from God.

Table of Contents

List of Tables

List of Figures

Chapter 1: Introduction

Burning behavior of solids is a still very active subject in fire research. Most work has focused on thermally thick solids and has generally ignored chemical kinetic effects of decomposition. Especially, the interest on polymers is continuously increasing due to their huge variety of use and the development of new materials. The introduction of nano-particles in polymers has produced materials with enhanced properties. One fruitful application of nano-particles has been the use of nano-clay to reduce the burning behavior of nylon. In that applications there have been questions about the mechanistic role of the clay and the extent of the improvement. Studies to examine these features have been troubled by the differing results according to thickness. Such results are systematically reported in a study by Liu[1] and Quintiere and Liu[2]. They used nylon (PA-6) and the nylon with the additive montmorillonite (MMT) clay. They showed that the behavior of thin materials was different than for that of thick materials, and its behavior was controlled by the kinetics of decomposition. However, the feature of the burning rate for thermally thick materials is quite different from that of the thermally thin materials. Particularly, the nylon with the clay formed the char crust on the sample surface which shields the sample from the external radiation and heat feedback from the flame, thus acting as a thermal insulation layer. Therefore, the nylon with the additive montmorillonite (MMT) clay significantly reduces the burning rate of the nylon sample. The accumulation of the initially well-dispersed clay particles in the sample on the burning surface is due to two possible mechanisms. One is recession of the polymer resin from the surface by decomposition. Clay particles tend to aggregate and stack against each other after the degradation of the organic treatment on the clay surface making them

more hydrophilic and less compatible with the resin. Another mechanism is the transportation of clay particles pushed by numerous rising bubbles of degradation products and the associated convection flow in the melt from the interior of the sample toward the sample surface[3]. The goal of this study is to predict the burning of thermally thin materials by modeling thermally thin burning behavior of a polymer. Specifically, the materials and the data of Liu[1] with nylon and 5% clay additive, conducted in the Cone Calorimeter will be used for comparison. To provide the needed data for the model, thermogravimetric analysis (TGA) and differential scanning calorimeter (DSC) analyses have been performed.

Generally, the burning behavior for nylon and the nano-composite with 5% clay as a function of thickness can be distinguished into the two kinds –thermally thick and thin. For thermally thick burning, steady burning is clearly indicated. This means the thermal depth of heat conduction into the solid will reach a constant value during steady state. In contrast, thermally thin burning displays a sharp peak condition in the burning rate. The conduction thermal wave reaching the back-face, due to pre-heating before ignition or later for a thicker sample, will encourage a uniform temperature across the solid's thickness and therefore, thermally thin burning. It is also seen that at low heat fluxes, the pre-heating of the sample before ignition causes thermally thin burning to mostly prevail for even physically thick samples. Despite steady burning exhibited for a thick sample, thin burning behavior can be seen at the end of burning for a well insulated back-face. It has been shown that thermally thin burning is governed by decomposition chemical kinetic properties, while thermally thick burning and particularly steady, non-charring burning is governed by the heat of gasification[2]

For the point of view of material flammability, the improvements due to the clay loading for the nano-clay composite are very satisfactory. First, the ignition time is increased,

which means during a real fire, the available evacuation time is increased. Second, the total amount of energy is not changing by adding clay, but the peak heat release rate is greatly reduced. This can lower the risk of flashover occurrence. This is an important factor for life safety[2].

The modeling of burning rate will require an estimation of the flame heat flux. It has been shown by Quintiere and Rhodes[4] that the flame heat flux for thermoplastic-like materials burning in the Cone Calorimeter can be constant. They found constant net flame heat fluxes for polymers of 20 kW/m^2 for nylon 6/6, 19 kW/m^2 for polyethylene, 11 kW/m^2 for polypropylene, and 28 kW/m^2 for black PMMA over external irradiation levels ranging from 0 to 90 kW/m^2[5].

Up to now, fire researchers have most exclusively relied on the heat of decomposition or its related property, the heat of gasification to characterize the burning rate. The chemical kinetic and thermodynamic properties derived from the TGA and DSC data, have been generally ignored. It is important to more completely understand the role of these decomposition effects in the burning of thermally thin material. Moreover, it is useful to see if these properties can be adequately measured for use in fire models. Demonstrating the role of these common TGA/DSC property data for fire hazard evaluation of a material can provide insight and improve testing efficiency. It has been revealed that the burning rate for non-charring materials would achieve a steady value if the sample were sufficiently thick. In steady burning, only the heat of vaporization is a factor in decomposition and no kinetic properties pertain. However, for the thin materials the kinetic effects are clearly important.

A method has been used to determine the specific heat of a material during thermal decomposition using a combination of DSC and TGA data obtained at the same heating

rate. The heat of decomposition is calculated simultaneously using the same data. Experimental data are presented for the specific heat of both the virgin and char components for some temperature ranges. The specific heat of the virgin and char was carried out using DSC. Also, it was necessary to know the weight loss of the material as a function of temperature at the same heating rate as the DSC scan. This was carried out by TGA. During the decomposition process, the power input to the DSC is distributed into sensible and latent components for the material which could be separately determined. The DSC data curve can be interpreted to represent heat of melting , decomposition, and so on[6]. Brian Y. Lattimer[7] used the apparent specific heat capacity from DSC data which includes the sensible and latent portions of the heat capacity. The apparent specific heat capacity of the material as a function of temperature can only be developed after corrections are made to the raw DSC data. These corrections include the heat capacity of the containers and the heat transfer between the sample and the inert surrounding gas. Detailed thermal and physical property data are required to determine the apparent specific heat capacity. This includes the density as a function of temperature, the specific heat capacity as a function of temperature for the virgin and decomposed states, and the heat of decomposition.

Nonetheless, there has been a controversy about the utility of TGA for predicting fire behavior. While thermogavimetric analysis is a useful tool for quantifying a solid's thermal stability, it has several limitations for application to fire conditions. TGA's relevance to fires has been questioned because typical TGA heating rates (between 0.1K/min and 30K/min) are much lower than can be encountered in fires (sometimes 100 K/min or greater). One difficulty associated with using higher heating rates in TGA is that the thermal lag between the sample temperature and the temperature of the

atmosphere increases with the heating rate, particularly because the decomposition process is often endothermic[8].

Many papers on decomposition kinetics of polymers have appeared in literature. In most studies, standard TGA equipment was used for the measurements. Two divergences among the studies are obvious. The first is in the choice of kinetics models used to describe the decomposition kinetic, and second is in values of the Arrhenius parameters obtained in the chosen model. A first order reaction model has been most often used to describe the kinetics. Instead of the simple first order model, several more complex models have been proposed. Unfortunately, these models usually have large number of parameters to fit, which make their practical use very difficult. For the Arrhenius parameters, the activation energy monotonously increases with the degree of conversion of material decomposed and with higher heating rate. A higher heating rate of course leads to decomposition at higher temperature. The reason why the activation energy changes with the degree of conversion and heating rate is the distribution of size of volatile products. As temperature increases, the size of volatiles increases. The pre-exponential factor also depends on the heating rate[8, 9].

This study will attempt to examine the use of TGA and DSC data in a thermally thin model for fire applications. The data will be used consistently in the model, and the model will then be examined for accuracy with data. The accuracy of the model will be assessed, and the applicability of the model for thermally thin conditions will be described. The variations in heating rates will be examined and related to the TGA/DSC conditions. A successful application of TGA/DSC data in predicting fire behavior can improve the use of such data to assess fire hazard potential of a material.

Chapter 2: Thermogravity Analysis

2-1. Introduction

2-1-1. General concept of TGA

Thermal analysis is the name given to the measurement of a sample as the sample is programmed through a predetermined temperature regime in a specified atmosphere. In the thermal analysis, a controlled temperature program means heating or cooling the sample at some predetermined and defined rate. Conventionally, thermal analysis experiments are carried out at a constant heating rate, and a property change is measured as a function of time (or temperature). The substance is usually studied in the condensed phase, i.e., solid or liquid, but a change from solid to gas or liquid to gas may be monitored; thus, the gas produced generally escaped from the system under study. At one atmosphere the gaseous environment may be stable or dynamic; that is, the gas may either not be changed during the experiments, or one may control the flow of gas over the sample. The atmosphere in such circumstances may be oxidative (i.e., air or oxygen) or inert (e.g., helium, argon, or nitrogen).

Thermogravimetry analysis is one of the thermal analysis techniques available for the characterization of the thermal properties of materials such as the activation energy (E_a)and the pre-exponential factor(a_p). The formal definition of thermogravimetry (TG is the preferred abbreviation, although TGA is also used) has been given by the Nomenclature Committee of the International Confederation for Thermal Analysis and Calorimetry (ICTAC) as “a technique in which the mass of a substance is measured as a

function of temperature whilst the substance is subjected to a controlled temperature programme". It is the most widely used experimental technique for determining the thermal change of solids. A high-precision scale is used to measure the mass loss of a very small sample. The sample is usually no more than a few mg and almost always less than 20 mg. It is exposed to an atmosphere with specified temperature and composition. Early TG experiments were conducted in constant temperature atmospheres, but modern experiments almost always expose the sample to an atmosphere having a temperature that increases linearly with time. The non-isothermal test method approach will be used here. To completely eliminate the heat transfer problem, the sample temperature is taken as equal to the temperature of the atmosphere[8].

In thermal decomposition, the mass of reactants disappears and forms gaseous products and possibly a residue of char. The record is the TG curve; the mass is normally plotted on the ordinate, decreasing down toward the origin, and temperature (T) or time (t) is on the abscissa, increasing from left to right according to the basic rules for plotting any kind of graph. The purpose is to determine the kinetic parameters of thermal decomposition of the material. A typical TGA curve is shown in Figure 2-1.

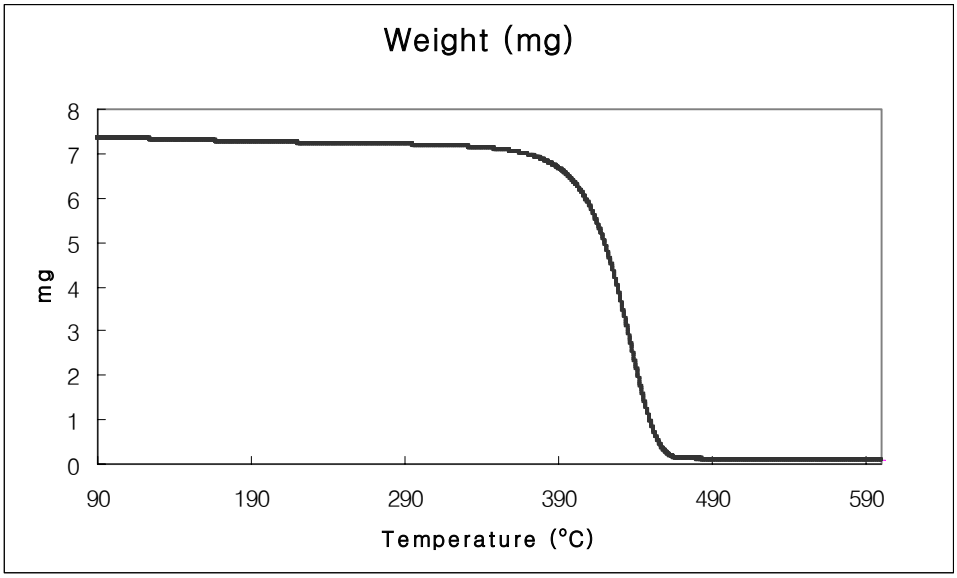

Figure 2-1. An example of typical TGA curve

2-1-2. Principle of the method

The form of the TG curve obtained experimentally is dependent on the interplay of two major factors: (1) the properties of the sample and (2) the actual experimental conditions used, also called procedural variables. Both factors can affect the kinetics of any reaction that take place, so that a change in either will have a subsequent effect on the form of the TG curve. It is also important to note that unless the sample is held at constant temperature, applying a heating rate produces nonequilibrium conditions. It is possible to calculate a theoretical TG curve if the kinetic mechanism and parameters are known, on the assumption that heat transfer is instantaneous and no temperature gradient exists within the sample. Thus the kinetics of most reactions under isothermal conditions can be summarized by the general equation

$$\frac{d\alpha}{dt} = kf(\alpha) \qquad (2\text{-}1)$$

Here α is the fraction reacted in time *t* and is equal to $\frac{m - m_i}{m_f - m_i}$, where m_i is the initial mass of the sample, m is the mass at time *t* and m_f is the final mass of the sample; k is the rate of reaction; and $f(\alpha)$ is some function of α .

The temperature dependence of the rate constant can be assumed to follow the Arrhenius equation: $k = a_p e^{-E_a/RT}$ (2-2)

where *T* is the absolute temperature, a_p is the exponential factor, E_a is the activation energy, and *R* is the gas constant.

the heating rate , $\beta \equiv \frac{dT}{dt}$ for a constant linear heating rate, (2-3)

Combination of equation (2-1) and (2-2) give

$$\frac{d\alpha}{dt} = a_p f(\alpha) e^{-E_a/RT} \qquad (2\text{-}4)$$

Substitution for d*t* using equation (2-3) gives

$$\frac{d\alpha}{dT} = \frac{a_p}{\beta} f(\alpha) e^{-E_a/RT} \qquad (2\text{-}5)$$

Which , if rearranged , provides

$$\frac{d\alpha}{f(\alpha)} = \frac{a_p}{\beta} e^{-E_a/RT} dT \qquad (2\text{-}6)$$

Equation (2-6) is the basic equation of the TG curve when it integrated. If the form of the function $f(\alpha)$ is known, integration of left-hand side of the equation is straightforward. The integration limits are between the initial and final temperature of the reaction, or between α =0 and α =1. The value of E_a and a_p have marked influence on the temperature range over which the TG curve is observed, but they do not influence the shape of the curve too greatly. However, the kinetic mechanism, the form of $f(\alpha)$ determines the shape of the curve.[10]

2-2. Theory for thermal decomposition

To explain the thermal decomposition of a solid, we need to appreciate the stoichiometry, the mass conservation, and the reaction rate of the decomposing material. The model for the process is assumed as follows: The decomposing solid is considered as a perfect mixture of original solid fuel (active species, a) and char (c). The char forms a matrix, filling the same volume of the original material. Gaseous fuel is generated within and flows through the solid under constant pressure. Darcy-flow is not considered, as cracks and porous char allow ease of flow. The chemical stoichiometry is given as follows:

m (g) original(active) solid → (1-X_c) m (g) gas + X_c m (g) char

Next, we consider the conservation of mass for the solid within the control volume in Fig.2-2.

$$\frac{dm}{dt} = -\dot{m}_g \qquad (2\text{-}7)$$

Equation (2-7) means that the rate of mass loss change of the solid in the control volume over time is equal to the rate of mass of fuel gas coming out. Namely, the mass in the

control volume decreases as much as fuel gas is produced through the thermal decomposition process.

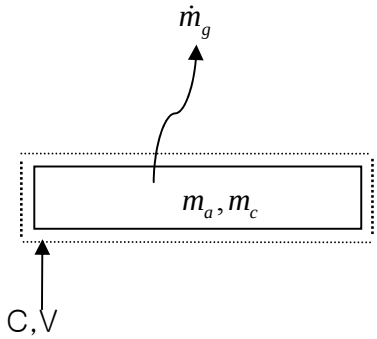

Figure 2-2. The control volume surrounding the decomposing material in TGA

Here, fuel active solid and residue (char) are in two-phase matrix.

Also, the total mass in a control volume during decomposition $m=m_a+m_c$, as the mass of the evolved gas is negligible. Lastly, the reaction rate is described in the equation (2-4); however, we need to determine the specific $f(\alpha)$. Actually, based on casual examination of literature data[11], it can be concluded that the reaction order does not deviate too far from unity, perhaps 0.5< n < 1.5 for most materials. Therefore, the thermal decomposition of the solid is assumed to follow a single-step first-order Arrehnius reaction. Therefore, the first order reaction is described by:

$$\dot{m}''' = \frac{1}{V}\frac{dm}{dt} = -\rho_a k(T) \qquad (2\text{-}8)$$

Because the char forms a matrix, filling the same volume of the original material, the volume, V is assumed fixed; that is, constant during the thermal decomposition. This ignores the possibility of swelling or shrinkage. Equation (2-8) tells us that the reaction

rate depends on temperature and is linear with the active species concentration, $\rho_a \equiv m_a / V$.

$$\frac{dm}{dt} = -m_a k(T) \tag{2-9}$$

Put in terms of conversion factor α defined before

$$\alpha = \frac{m - m_i}{m_f - m_i} = \frac{m/m_i - 1}{X_c - 1} \tag{2-10}$$

$$\frac{d\alpha}{dt} = \frac{1}{(m_f - m_i)} \frac{dm}{dt} \tag{2-11}$$

where $X_c = \frac{m_f}{m_i}$, called char fraction,

By stoichiometry of the decomposition reaction,

$$\frac{dm_a}{dt} = \gamma_a \left(-\dot{m}_g\right) \tag{2-12}$$

where as γ_a is the mass of active material /mass of original material lost, $\gamma_a = \frac{1}{1 - X_c}$

Combination of Equations (2-7) and (2-12) gives

$$\frac{dm_a}{dt} = \frac{1}{1 - X_c} \frac{dm}{dt} \tag{2-13}$$

Integrating Equation (2-13) over m, m_a.

$$\int_{m_a}^{0} dm_a = \int_{m}^{m_f} \frac{dm}{1-X_c}$$

$$-m_a = \frac{m_f - m}{1-X_c} \tag{2-14}$$

Combination of Equations (2-10) and (2-14) gives

$$-m_a = \frac{(1-\alpha)(m_f - m_i)}{(1-X_c)} \tag{2-15}$$

Combination of Equations (2-9), (2-11), and (2-15) gives

$$\frac{d\alpha}{dt} = \frac{(1-\alpha)}{(1-X_c)} k(T) \tag{2-16}$$

Conclusively, the specific $f(\alpha)$ is determined as described below.

$$f(\alpha) = \frac{(1-\alpha)}{(1-X_c)} \tag{2-17}$$

Also, we express Equation (2-17) substituting Equation (2-2) as follows.

$$\frac{d\alpha}{dt} = \frac{(1-\alpha)}{(1-X_c)} a_p e^{-E_a/RT} \tag{2-18}$$

This is the basic equation need in our TGA analysis to determine the kinetic parameters a_p and E_a.

2-3. Experimental data

Thermogravity analysis (TGA) was conducted for composites, pure nylon 6 and 5% additive montmorillonite (MMT) clay with nylon (PA-6). Pure nylon is also called polyamide 6. The molecular weights of PA 6 and PA 6 with MMT of 5% by mass fraction are 15,000 g/mol and 18,000 g/mol respectively[12]. The 5% sample has been formed as a nanocomposite in which there is a specific interaction between the clay and the polymer. Samples of about 5mg in the shape of powder and fragment were tested by TGA. To get complete experimental data needed for estimating a_p and E_a, TGA was conducted with a variety of heating rate, 1℃/min, 2℃/min, 5℃/min and 10℃/min. Also, we used different TGA of equipment; that is, TGA and DSC data were taken at VTEC laboratories in Bronx, NY and at FAA (Federal Aviation Administration) Technical center in Atlantic City. Also, some of TGA data are from Kashiwagi, NIST [13] . All of the TGA experiments conducted or taken are presented in Tables 2-1 and 2-2.

Table 2-1. Experiments conducted for TGA of Nylon

Nylon			
Laboratories	Heating rate (initial mass, m_i)	specimen	source
VTEC	5 ℃/min (5 mg), 10 ℃/min (5.4 mg)	Powder	Present
FAA	5 ℃/min (7.3 mg)	Fragment	Present
NIST	1 ℃/min (16 mg), 2 ℃/min (16.2 mg), 5 ℃/min (15.8 mg)	Powder	[13]

Table 2-2. Experiments conducted for TGA of Nylon+5%

Nylon+5%			
Laboratories	Heating rate (initial mass, m_i)	Specimen	
VTEC	2 ℃/min (5.7 mg), 5 ℃/min(5.5 mg), 10 ℃/min (5.2 mg)	Powder	present
FAA	5 ℃/min (4.5 mg)	Fragment	present
NIST	1 ℃/min (18.1 mg), 2 ℃/min (17.7 mg), 5 ℃/min (16.7 mg)	Powder	[13]

Also, all of the data are presented in Figures 2-3 and 2-4.

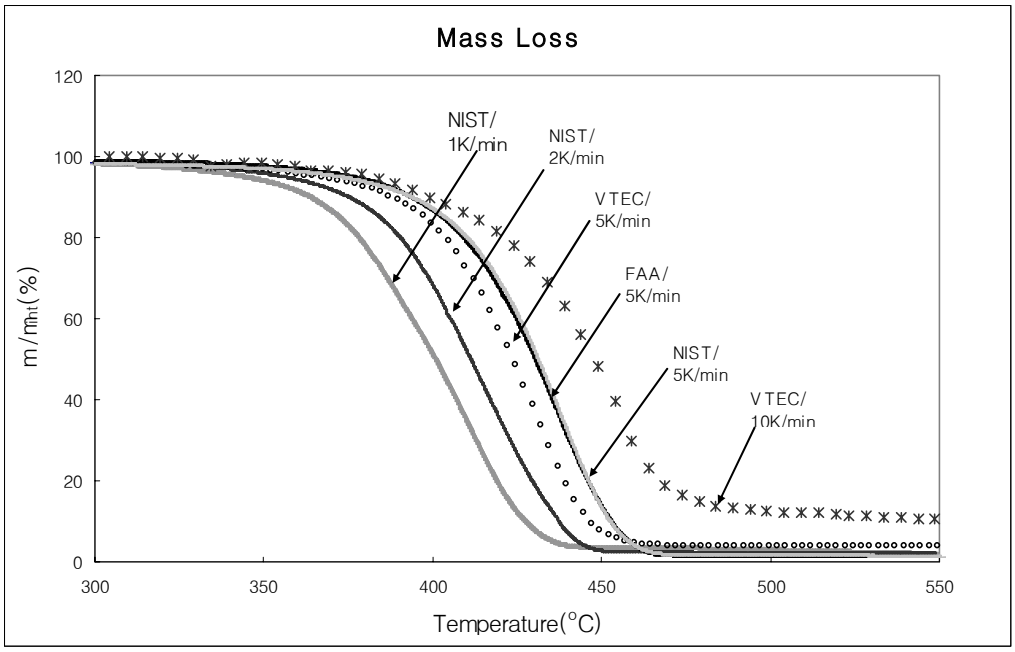

Figure 2-3. TGA curve of Nylon

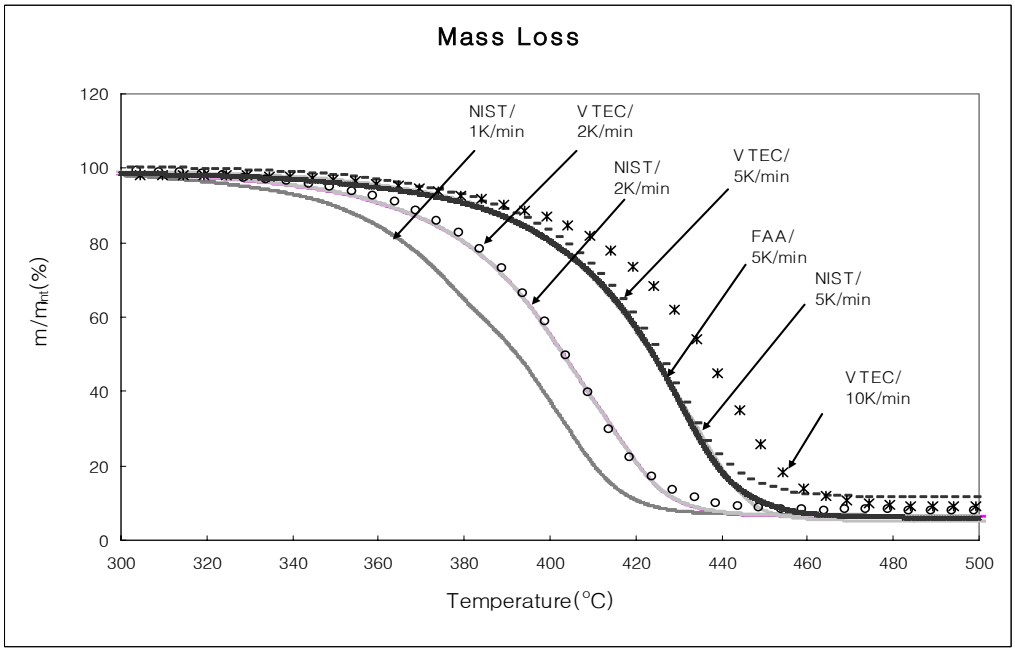

Figure 2-4. TGA curve of Nylon +5% clay

2-4. Analysis to determine a_p and E_a

In this section, the method to determine the kinetic parameters is discussed. Take the natural logarithms on both sides of the equation (2-18).

$$\ln\left(\frac{d\alpha}{dt}\right) = \ln\left(f(\alpha)a_p\right) - \frac{E_a}{R}\left(\frac{1}{T}\right)$$

$$\ln\left(\frac{d\alpha}{dt}\right) = \ln\left\{\frac{(1-\alpha)}{(1-X_c)} \times a_p\right\} - \frac{E_a}{R}\left(\frac{1}{T}\right) \qquad (2\text{-}19)$$

By plotting $\frac{d\alpha}{dt}$ against 1/T for selected value of α_i as taken from the TGA, the slope($-E_a / R$) from Equation (2-19) can be determined.

Then E_a and a_p are easily calculated.

$$E_a = -R \times slope \qquad (2\text{-}20)$$

$$a_p = \frac{\exp(\text{intercept})}{f(\alpha)} \qquad (2\text{-}21)$$

If E_a and a_p remain fairly invariant regardless of the data choice for α_i, then the model is a good fit.

In order to get the activation energy E_a and pre-exponential factor a_p, $\frac{d\alpha}{dt}$ must be computed from our TGA data.

Since α is defined as $\alpha = \frac{m - m_i}{m_f - m_i}$

$$\frac{d\alpha}{dt} = \frac{1}{m_f - m_i}\frac{dm}{dt}$$

TGA data shows mass fraction as a function of temperature, and temperature is a function of time.

$$\frac{dm}{dt} = \frac{dm}{dT}\frac{dT}{dt} = m_i \frac{d\frac{m}{m_i}}{dT}\frac{dT}{dt}$$

Where $\frac{dT}{dt}$ is the heating rate, β.

$\frac{-d\frac{m}{m_{\text{int}}}}{dT}$ is the derivative of weight (%/℃), directly from TGA data as shown in Figure 2-6.

$$\frac{d\alpha}{dt} = \frac{m_{\text{int}}}{m_f - m_{\text{int}}}\frac{d\frac{m}{m_{\text{int}}}}{dT}\frac{dT}{dt} \qquad (2\text{-}22)$$

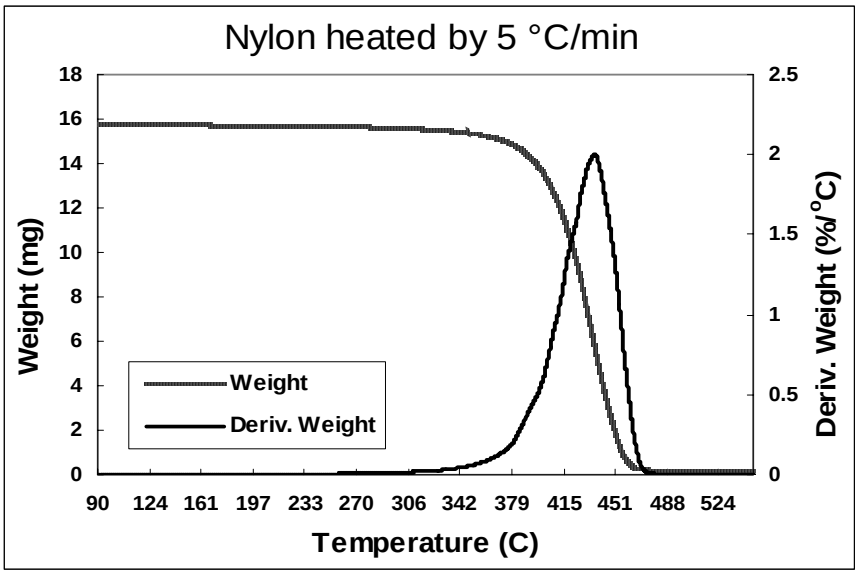

Figure 2-5 TGA data Nylon heated by 5℃/min

The process of executing consists of several steps. First, find the char fraction for $X_c = \frac{m_f}{m_i}$ for either Nylon and Nylon+5% clay, and substitute it into equation (2-17).Then $f(\alpha)$ is easy calculated for three different values α_i. Read the slope and intercept in Figure 2-6 and 2-7.

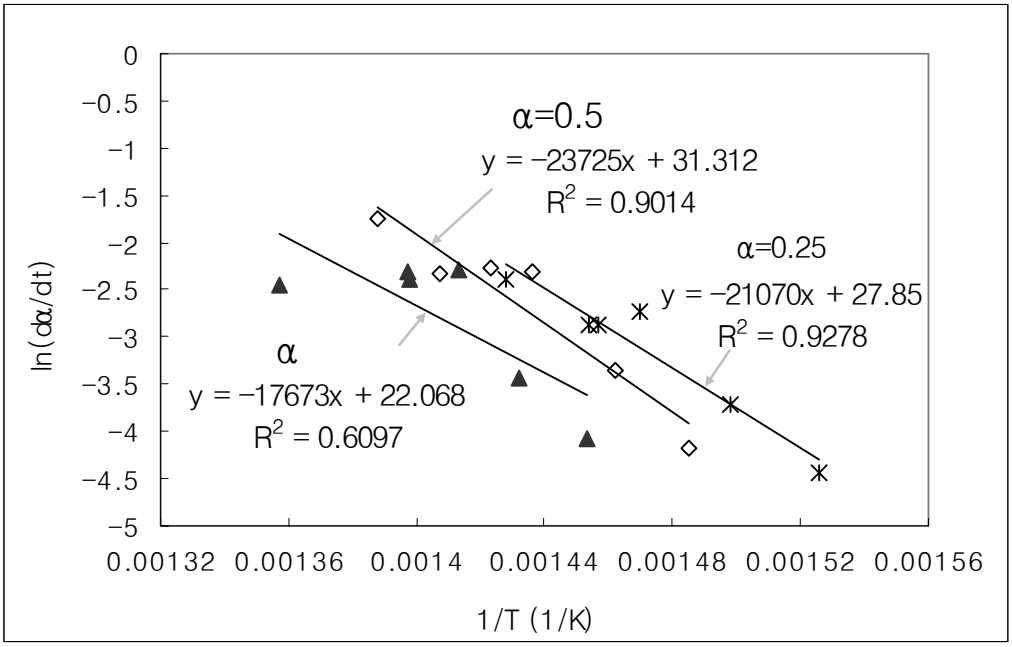

Figure 2-6. Determining E_a and a_p of Nylon using FAA, VTEC, and NIST data.

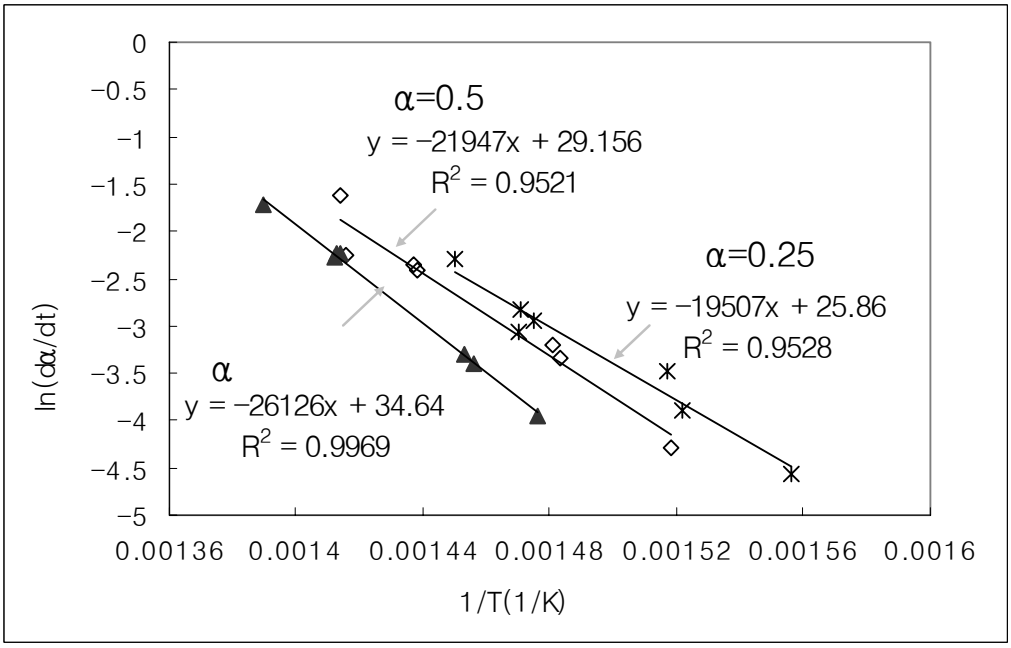

Figure 2-7. Determining E_a and a_p of Nylon+5% using FAA, VTEC, and NIST data.

Use the slope in equation (2-20) to get E_a, and use the intercept in equation (2-21) to get a_p. However, we can observe that the VTEC data are deviated from other data in the Figures 2-6 and 2-7. Hence, E_a and a_p are obtained again using FAA and NIST data.

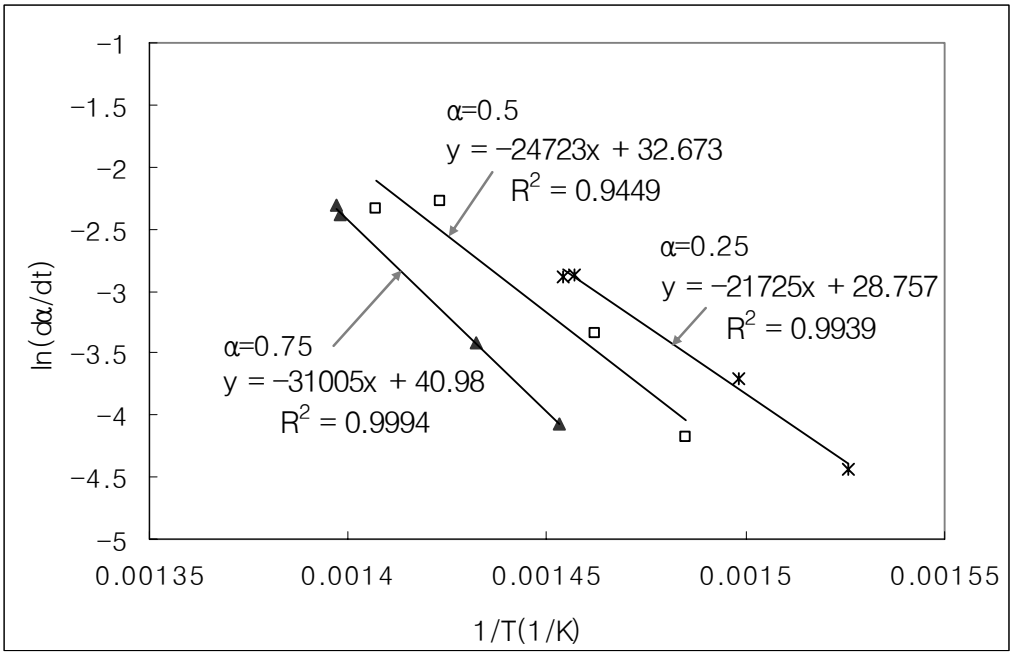

Figure 2-8. Determining E_a and a_p of Nylon using FAA and NIST data.

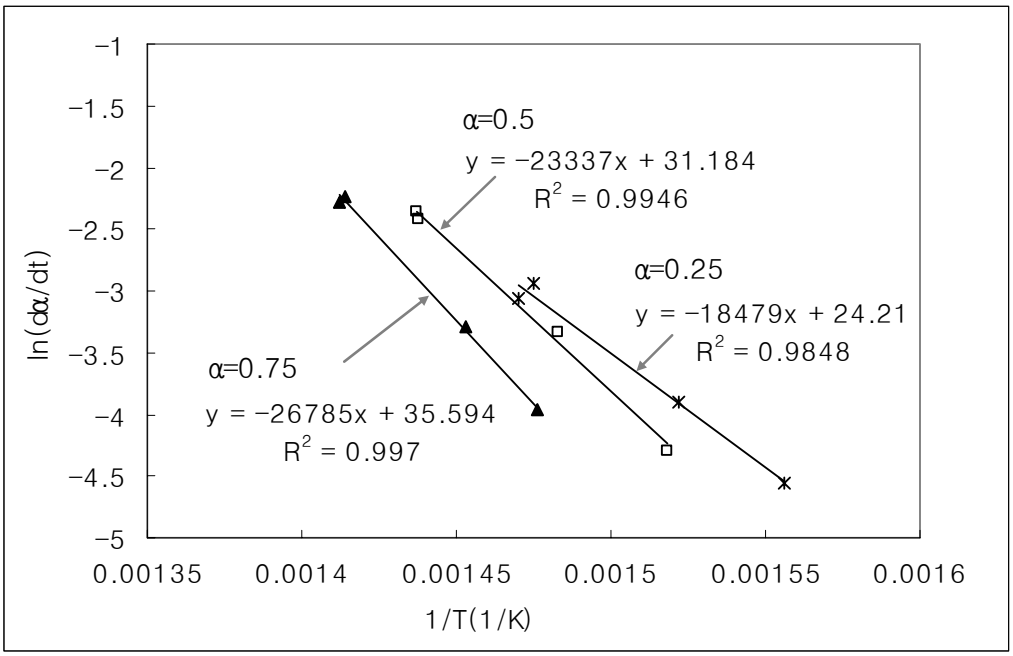

Figure 2-9. Determining E_a and a_p of Nylon using FAA and NIST data.

Those values from Figures 2-8 and 2-9 are listed in table 2-3.

Table 2-3. Kinetic parameter using FAA and NIST data

Nylon X_c=0.016					
α	slope	intercept	E_a (J/mol)	f(α)	a_p
0.25	-21725	28.76	181	0.762195	4.05E+11
0.5	-24723	32.67	206	0.50813	3.05E+13
0.75	-31005	40.98	258	0.254065	2.47E+11
Nylon+5% clay X_c=0.05					
α	slope	intercept	E_a (kJ/mol)	f(α)	a_p
0.25	-18479	24.21	154	0.7895	4.14E+11
0.5	-23337	31.18	194	0.5263	6.63E+14
0.75	-25785	35.59	223	0.2632	1.09E+15

As the values for E_a and a_p are not constant for each of the α_i data selected, the assumption of a first order reaction is not perfect. However, without a full understanding of the chemical decomposition reaction, it is the most reasonable approximation to the process. But the best choice of E_a and a_p is not directly apparent from Table 2-3.

A refinement in the fitting process is performed by using the range of the parameters in Table 2-3 together with an exact solution of the basic TGA Equation (2-18) gives

$$\alpha = 1 - e^{-AF[T]}$$

where $F[T] = \int_{T_\infty}^{T} e^{-E_a/RT} dT$

and $A = \dfrac{-a_p}{(1 - X_c)\beta}$

Substitute $\alpha = \dfrac{m - m_i}{m_f - m_i} = \dfrac{m/m_i - 1}{X_c - 1}$ into the above equation

$$\frac{m}{m_i} = X_c - \exp\left[-\frac{a_p}{(1 - X_c)\beta} \int_{T_\infty}^{T} \exp(-E_a/RT) dT \right] (X_c - 1) \qquad (2\text{-}23)$$

By selecting refined values for E_a and a_p, the theoretical solution was "best" matched to the experimental data. The best choices of E_a and a_p are given as the Table 2-4.

Table 2-4. Kinetic parameters

	Activation energy(E_a)	Pre-Exponential factor(a_p)
Nylon	223kJ/mol	1.5×10^{14}
Nylon+5%	223kJ/mol	2.1×10^{14}

The degree of fit to the experimental results is shown in Figures 2-10 and 2-11.

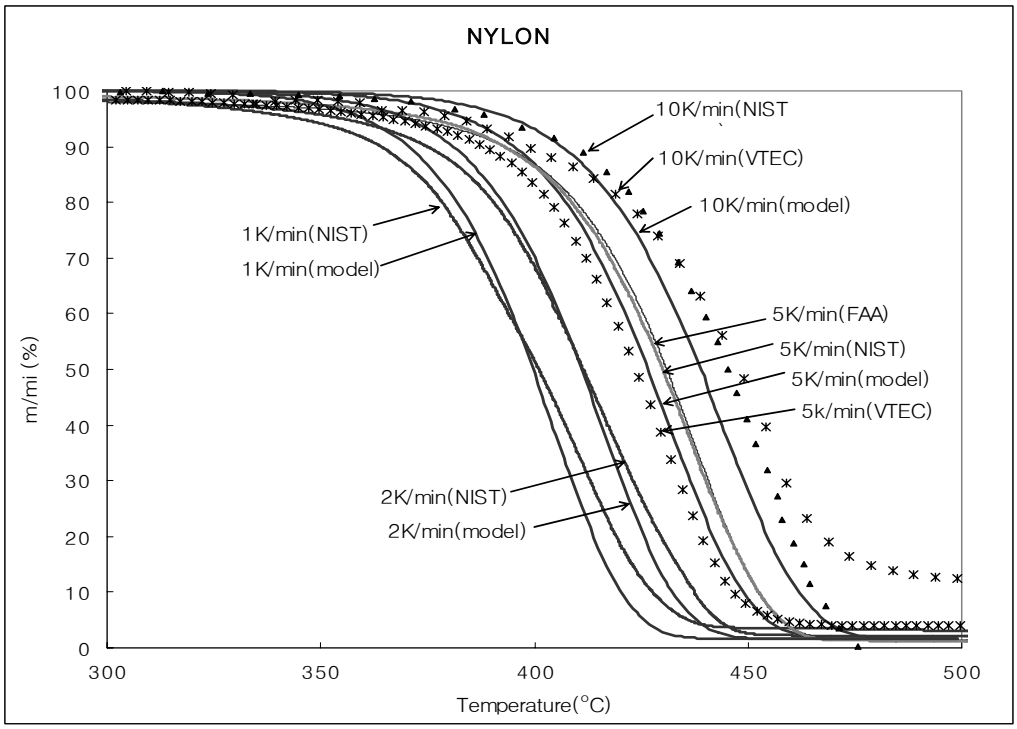

Figure 2-10. Comparing the model to the experimental data for Nylon in terms of mass conversion.

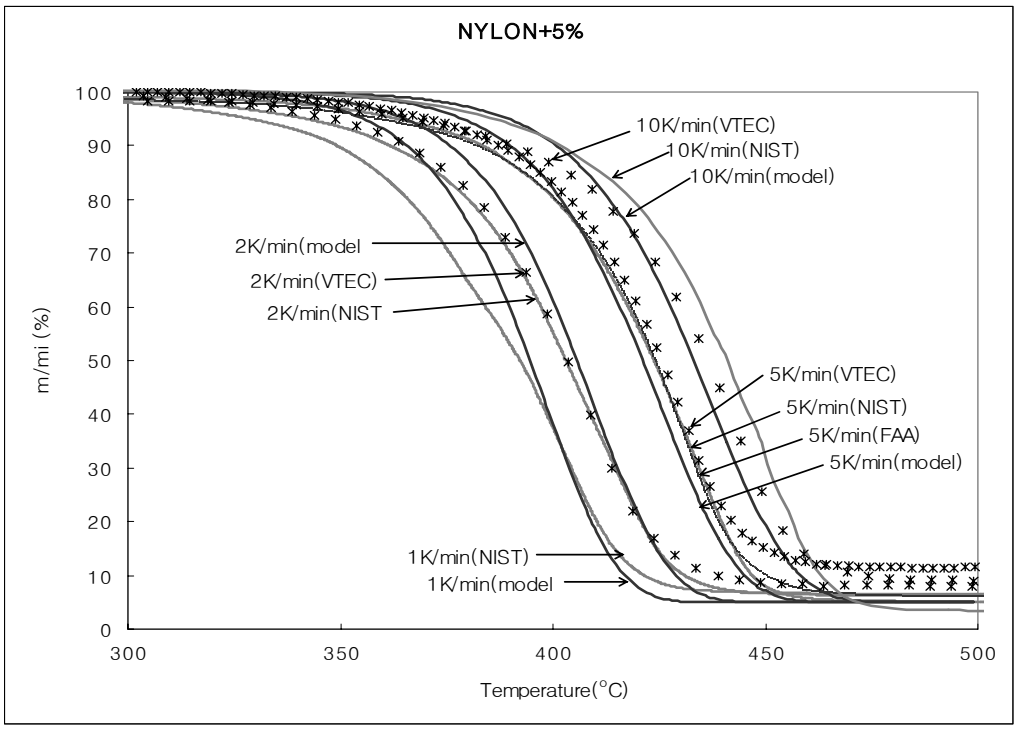

Figure 2-11. Comparing the model to the experimental data for Nylon+5% clay in terms of mass conversion.

The degree of fit to the rate of decomposition curves is also shown in Figures 2-12 and 2-13.

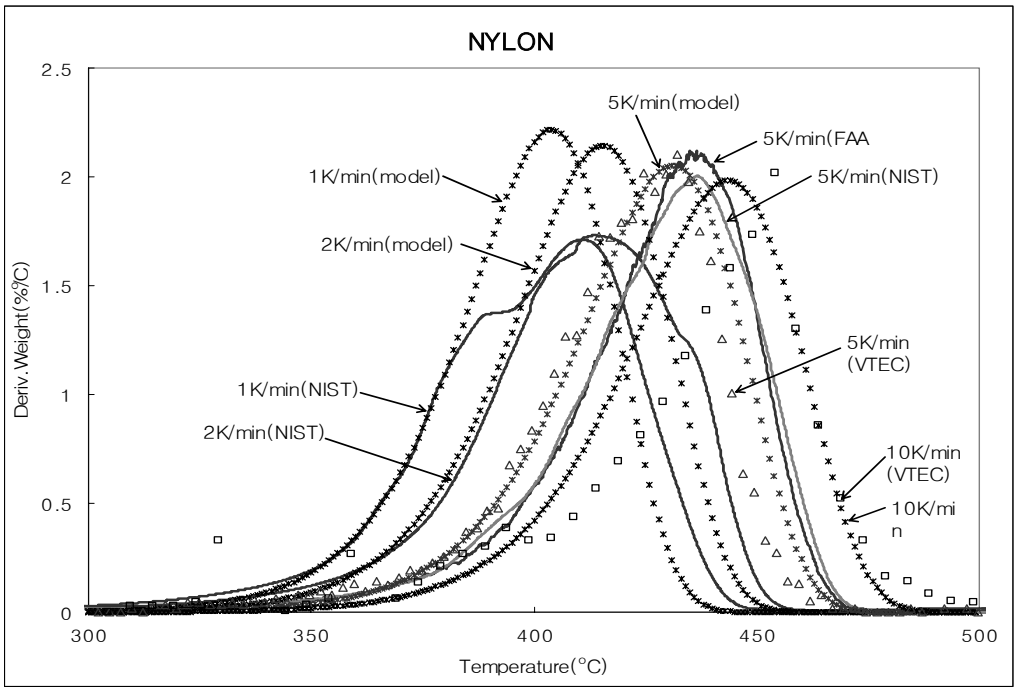

Figure 2-12. The rate of decomposition curves of Nylon.

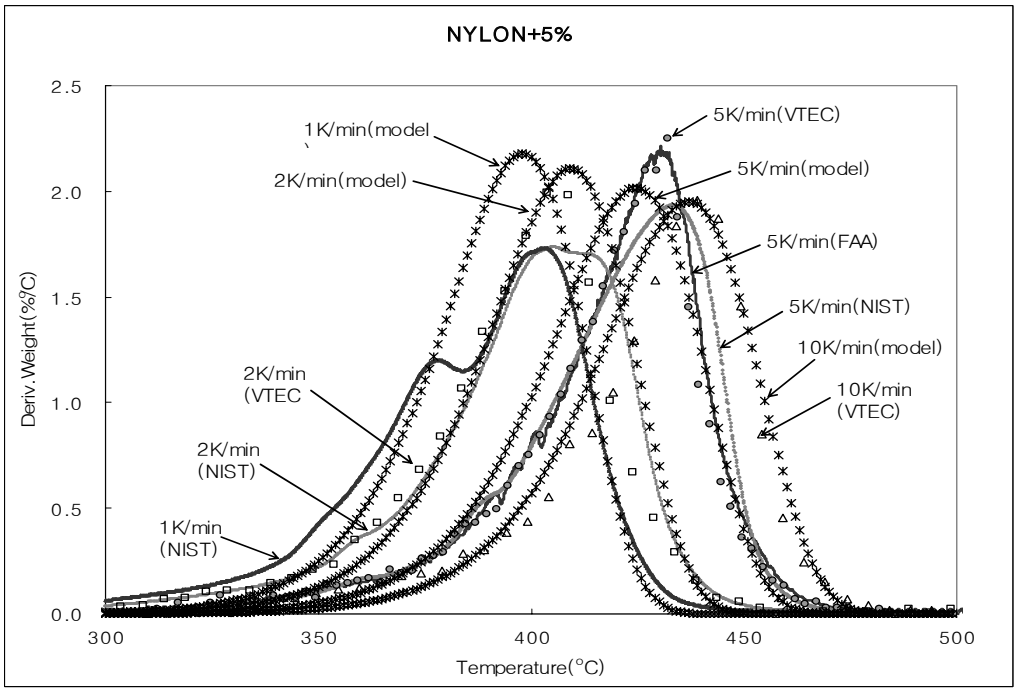

Figure 2-13. The rate of decomposition curves of Nylon+5% clay.

Chapter 3: Differential Scanning Calorimetry

3-1.Introduction

Differential scanning calorimeter (DSC) measures the difference in energy inputs into a substance and reference material as a function of temperature while the substance and reference are subjected to a controlled temperature program. The "differential" indicates the difference in behavior between the material under study and a supposedly inert reference material. In this manner the temperature at which any event either absorbs or releases heat can be found. This allows the determination of, e.g., phase transition temperature and the study of chemical reaction. Similarly, heat capacity measurements can be performed. That is, it tells us the change of enthalpy of material under the temperature program. By careful calibration and analysis, DSC data can yield the specific heat and heat of phase changes of a material as a function of temperature. The temperature program in the DSC is similar to that of TGA as constant heating rates are generally used.

Two modes, power compensation differential scanning calorimetry (power compensation DSC) and heat-flux differential scanning calorimetry (heat-flux DSC), can be distinguished, depending on the method of measurement used. A system with multiple sensors (e.g., a Calvet-type arrangement) or with a controlled heat leak (Boersma-type arrangement) would be heat –flux DSC. In 1955, Boersma recommended removing the thermocouple of the sensors from direct contact with the samples and introducing a controlled heat leak between the sample and the reference containers. In subsequent years this arrangement has come to be referred to as "heat –flux DSC". In 1964, the Perkin-

Elmer Corporation developed and patented a differential scanning calorimeter that involved separate heaters for the sample and reference containers with the differential power needed to keep the sample and the reference at the same temperature measured directly. This technique is currently referred to as “power-compensated DSC”[10]. As a result, the brief designation DSC is often used without clarification for both methods. Our DSC was conducted on a Perkin Elmer DSC7 in FAA in Atlantic city and a NETZSCH STA 409 PC Luxx in VTEC laboratory in Bronx NY. Those DSC apparatuses belong to power compensation differential scanning calorimetry.

Figure 1 shows a schematic of a typical DSC apparatus for one sample. Two samples on cups are used: one cup contains the sample to be measured, and the other cup may contain a reference sample or can be empty. The output of the DSC is the difference in power supplied to the sample cup and the reference cup.

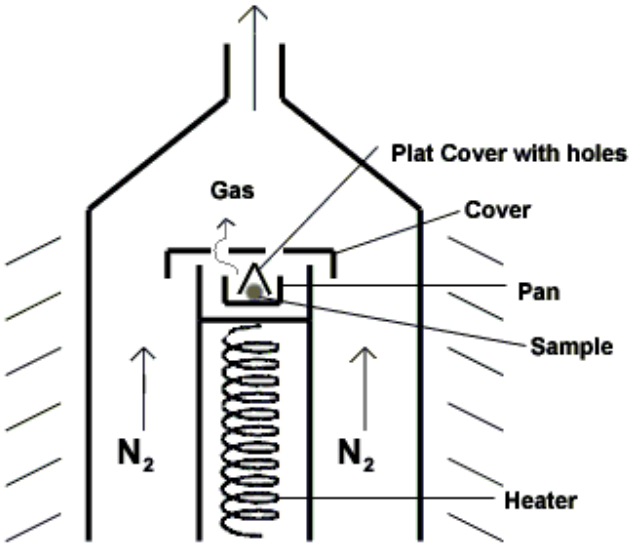

Figure 3-1. Schematic of one pan

3-2. Theoretical basis of DSC data

We shall now show how the output power signal of the DSC can be interpreted as the sample specific heat, heat of melting, heat of vaporization or decomposition. The interpretation will ultimately rely on a careful procedure involving the establishment of a "baseline" signal for no sample, and a special procedure to evaluate the heat loss between the heater-cup system and flowing gas. The gas is commonly inert. Figure 3-2 shows a schematic for one cup.

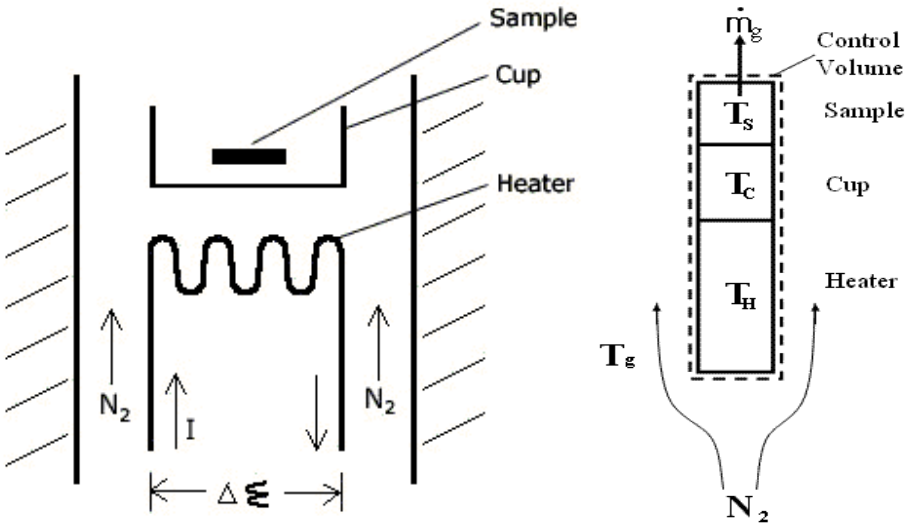

Figure 3-2. Schematic of heat transfer in DSC

A conservation of energy applied to the control volume of Figure 3-2 will yield in general.

$$\sum_i \frac{d}{dt}(m_i h_i) + \dot{m}_g h_g = -\dot{q}_L + \dot{q} \qquad (3\text{-}1)$$

where $\dot{q}_L$ is the heat loss to the flowing gas

$\dot{m}_g$ is the rate of gas evolved from the sample

h_g is the enthalpy per unit mass of gas

$m_i h_i$ is the enthalpy of the heater, cup, or sample

$\dot{q}$ is the electric power supplied to the heater, $I \cdot \triangle \varepsilon$.

3-2-1 Empty cup systems

First apply Equation (3-1) to a system of two empty cups as shown in Figure 3-3. As the mass of the heater and cup are constant, and they can be taken at the same temperature, Equation (3-1) becomes

$$C\frac{dT}{dt} = -\dot{q}_L + \dot{q} \qquad (3\text{-}2)$$

for each cup system. Here C represents the heat capacity (mc) of the cup and heater.

The programmed temperature for a DSC will give the same temperature for each cup over time. Thus, the difference in power supply to the two empty cups, designated by subscripts 1 and 2, is

$$\triangle\dot{q} = \triangle\dot{q}_2 - \triangle\dot{q}_1$$

$$= (C_2 - C_1)\frac{dT}{dt} + (\dot{q}_{L,2} - \dot{q}_{L,1}) \qquad (3\text{-}3)$$

The first term on the right-hand-side is the “baseline” correction and the second term is the heat loss correction, $\triangle\dot{q}_L$.

The heat loss, especially by convection, can be taken as linear in temperature, T, as

$$\dot{q}_L = (T - T_g)/R \qquad (3\text{-}4)$$

where R is the thermal resistance. Generally programmed temperature rise in time is taken as a constant linear value, similar to TGA rates. However, if the rate is frozen at several fixed temperatures, a steady-state signal will be the output. This is illustrated in Figure 3-3.

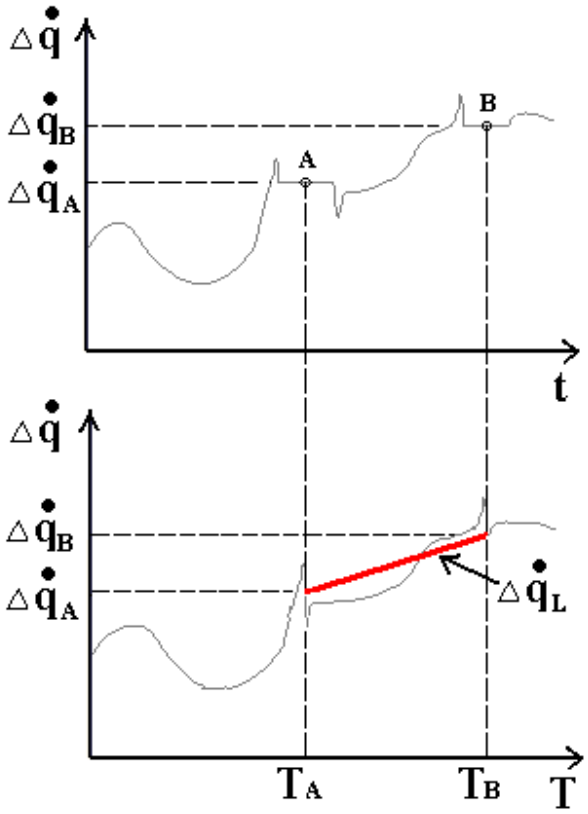

Figure 3-3. Heat losses

Two temperatures, T_A and T_B, are illustrated where the system was allowed to achieve a steady state in which $\frac{dT}{dt} = 0$. Hence, the signal output would give the heat loss correction at those temperatures, e.g.,

$$\triangle\dot{q} = \triangle\dot{q}_L = \dot{q}_{L,2} - \dot{q}_{L,1} \tag{3-5}$$

Assuming constant R between T_A and T_B, $\triangle\dot{q}_L$ can be taken as linear over T.

Once the $\triangle\dot{q}_L$ convection has been approximated over the relevant range of T, the "baseline" heat capacities can be determined for the empty cups, i.e.,

$$(C_2 - C_1)\frac{dT}{dt} = \triangle\dot{q} - \triangle\dot{q}_L \tag{3-6}$$

3-2-2 Sample systems

Now a sample is placed in one of the cups, and the same programmed heating rate is repeated. As the heat loss correction may have changed, this measurement is repeated for the sample system. Consider the enthalpy change for the sample with three considerations.

1. inert sample

2. melting sample

3. decomposing sample to char and vapor

1. Inert sample

Let mh designate the enthalpy of the sample. For an inert sample mass, m, does not change, so that

$$\frac{d}{dt}(mh) = m\frac{dh}{dt} = mc\frac{dT}{dt} \tag{3-7}$$

where c is the specific heat of the sample, or $C \equiv mc$ is the total heat capacity.

2. Melting sample

Designate the phase change as from the original solid(s) to the liquid (l). At the melt temperature, T_m, the mass of the sample can be both solid and liquid.

$$m = m_s + m_l$$

But as m is constant,

$$\frac{dm_s}{dt} = -\frac{dm_l}{dt}$$

Then, as T_m is constant,

$$\frac{d(mh)}{dt} = \frac{d}{dt}(m_s h_s + m_l h_l)$$

$$= \frac{dm_s}{dt}h_s(T_m) + \frac{dm_l}{dt}h_l(T_m) + mc\frac{dT}{dt}$$

$$= \left(-\frac{dm_s}{dt}\right)(h_l - h_s) + mc\frac{dT}{dt}$$

where $h_l - h_s$ is the enthalpy change at melting or the "heat of melting" designated as Q_m.

$$\frac{d(mh)}{dt} = \left(-\frac{dm_s}{dt}\right) Q_m + mc\frac{dT}{dt} \tag{3-8}$$

3. Decomposing sample

The sample is considered to have the stoichiometry as follows:

$$1\text{g Active}(a) \longrightarrow (1 - X_c)\,\text{g Vapor}(g) + X_c\,\text{g Char}(c)$$

The active species could be liquid or solid. The enthalpy per unit mass of each species is given in terms of its heat of formation ($\triangle h^o_{f,i}$) as

$$h_i = \triangle h^o_{f,i} + \int_{25^oC}^{T} c_{p,i}\,dT \tag{3-9}$$

Use Figure 3-4 to designate the control volume for the specimen.

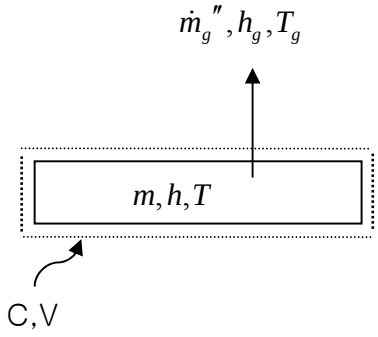

Figure 3-4. Control volume surrounding the specimen

As in the TGA analysis, the control volume contains char and active species, but no accumulation of vapor. Therefore, by conservation of mass

$$\frac{dm}{dt} = \frac{d(m_a + m_c)}{dt} = -\dot{m}_g \tag{3-10}$$

By conservation of species and stoichiometry,

$$\frac{dm_c}{dt} = -X_c \frac{dm_a}{dt} \tag{3-11}$$

Conservation of energy gives, from Equation (3-1),

$$\frac{d(mh)}{dt} + \dot{m}_g = \dot{q} \tag{3-12}$$

where $\dot{q}$ is the net heat added. The left-hand-side (LHS) can be rearranged using Equation (3-9), (3-10), and (3-11) as

$$LHS = (m_a c_a + m_c c_c)\frac{dT}{dt} + \frac{dm_a}{dt} h_a - X_c \frac{dm_a}{dt} h_c - (1 - X_c)\frac{dm_a}{dt} h_g$$

$$= C\frac{dT}{dt} + \left(-\frac{dm_a}{dt}\right)\left[-h_a + X_c h_c + (1 - X_c)h_g\right] \tag{3-13}$$

The heat of decomposition taken as a positive number when endothermic reaction is defined at 25℃ by

$$Q_p(25^o C) \equiv X_c \triangle h^o_{f,c} + (1 - X_c)\triangle h^o_{f,g} - \triangle h^o_{f,a} \tag{3-14}$$

in terms of the heats of formation. From Equation (3-9) at any temperature, T ,

$$Q_p(T) = X_c h_c + (1 - X_C) h_g - h_a$$

$$= Q_p(25^o C) + X_C \int_{25}^{T} c_{p,c} dT + (1 - X_C) \int_{25}^{T} c_{p,g} dT - \int_{25}^{T} c_{p,a} dT \quad (3\text{-}15)$$

The energy equation can then be expressed by

$$C \frac{dT}{dt} + \left(- \frac{dm_a}{dt} \right) Q_p(T) = \dot{q} \quad (3\text{-}16a)$$

or

$$C \frac{dT}{dt} + \left(- \frac{dm/dt}{(1 - X_c)} \right) Q_p(T) = \dot{q} \quad (3\text{-}16b)$$

Note, the heat of decomposition in the equation is that taken at the temperature where decomposition occurs.

3-3. Interpretation of DSC data

Several steps are needed in the processing of DSC data in order to extract accurate thermodynamic properties. First, the power difference signal for two empty cups must be corrected for the heat loss. The results gives the "baseline" heat capacity of the empty cups. From Equation (3-3)

$$(C_2 - C_1) \frac{dT}{dt} = (\triangle \dot{q} - \triangle \dot{q}_L)_{cups} \quad (3\text{-}17)$$

This process is illustrated in Figure 3-5.

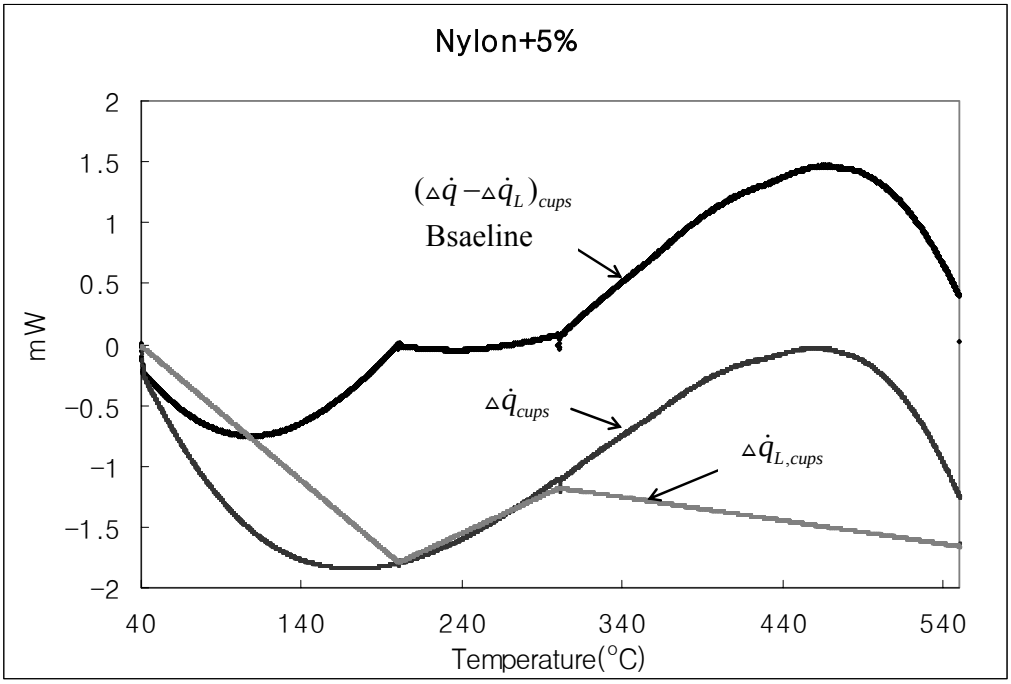

Figure 3-5. Power supplied to two empty cups; baseline determined

Second, a sample is placed in one cup and programmed at the same heating rate. The heat loss correction is also applied again. The net signal output is determined as $(\triangle\dot{q}-\triangle\dot{q}_L)_{cups+sample}$. This is illustrated in Figure 3-6.

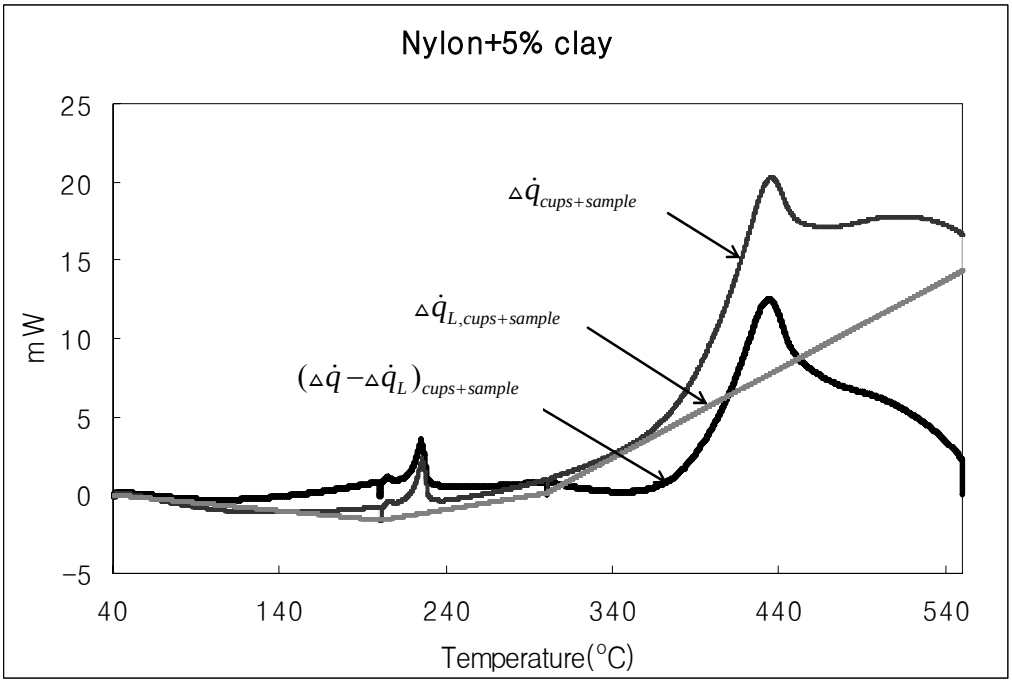

Figure 3-6. Power supplied to the sample placed in one cup and the other empty cup; baseline plus sample power determined.

Finally, the two corrected signals are subtracted to leave the effect of only the sample. This is illustrated in Figure 3-7. That signal is then needed to determine the sample the sample properties.

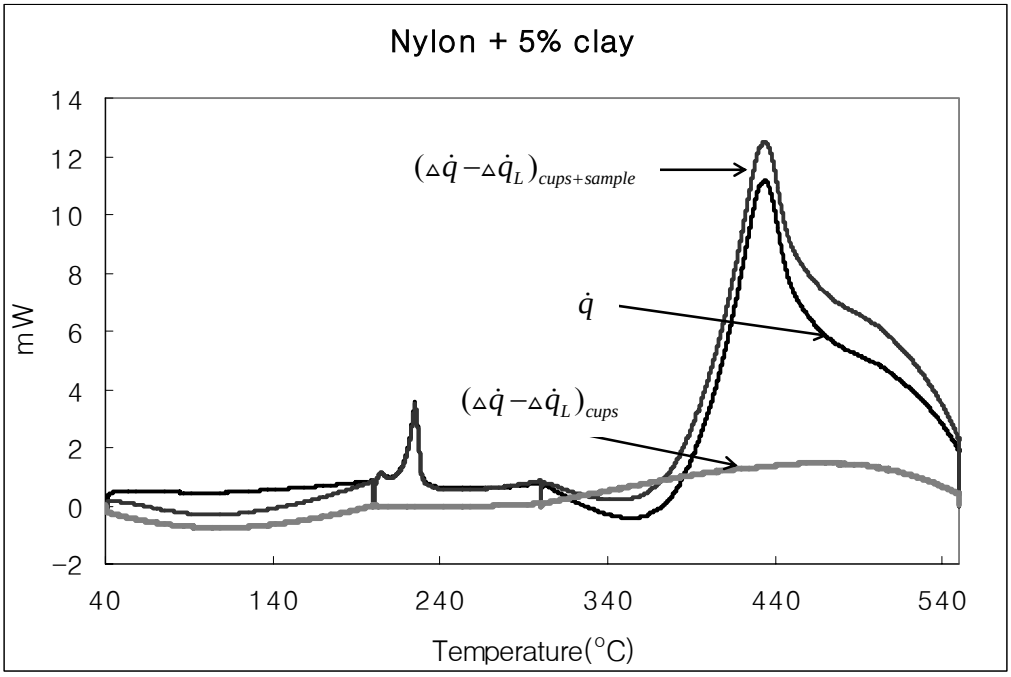

Figure 3-7. Power supplies to the sample

Let the sample signal be designated as

$$\dot{q} \equiv (\triangle\dot{q}-\triangle\dot{q}_L)_{cups+sample} - (\triangle\dot{q}-\triangle\dot{q}_L)_{cups} \tag{3-18}$$

In Figure 3-6 and 3-7, slight negative bumps occurs for the temperatures between 300 ℃ to 400 ℃. These suggest exothermic decomposition and not incredible, and these attribute them to experiment inaccuracy.

For the same heating rates, the cup heat capacity terms will cancel. The sample signal can then be related to the following:

1. Inert sample

$$\dot{q} = C\frac{dT}{dt} \tag{3-19a}$$

2. Melting sample

$$\dot{q} = \left(-\frac{dm_s}{dt} \right) Q_m + mc\frac{dT}{dt} \tag{3-19b}$$

3. Decomposition sample

$$\dot{q} = C\frac{dT}{dt} + \left(\frac{-dm/dt}{(1-X_c)} \right) \triangle h_d \tag{3-19c}$$

For a constant heating rate, $\beta = \frac{dT}{dt}$, the signal can be expressed as a specific heat term,

$$c = \frac{\dot{q}}{m_i \beta} \tag{3-20}$$

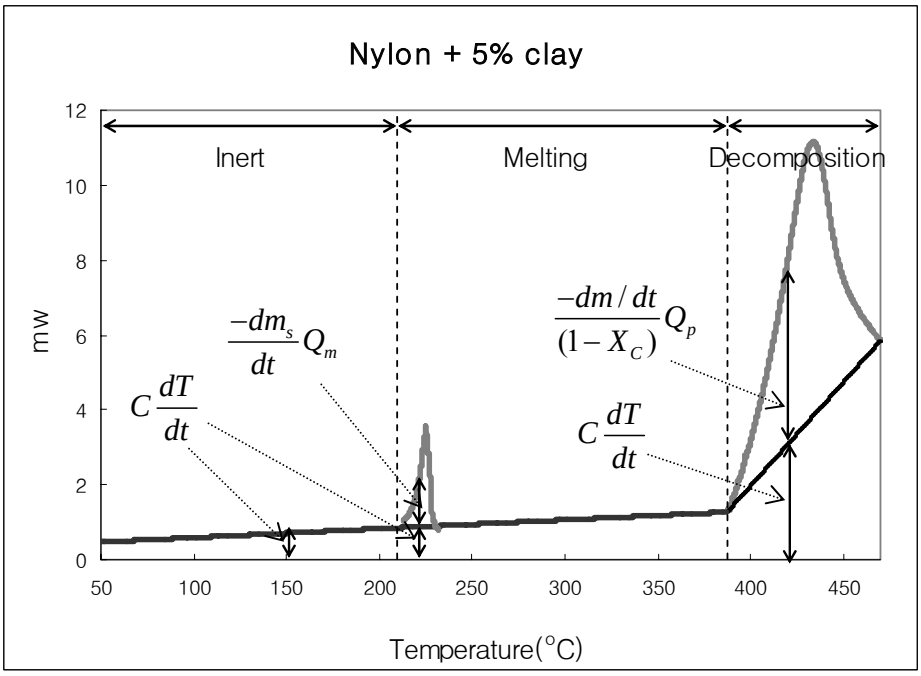

Figure 3- 8. Sample signal of Nylon+5% clay at $\beta = 5^o C/\min$.

Up to T_m=200 ℃, $c = \dfrac{\dot{q}}{m\beta}$

At T_m, the bump gives the heat of melting. This can be seen from Equation (3-19b). Re-write as

$$c_{eff} = \frac{\dot{q}}{m\beta} = -\frac{dm_s}{mdT}\frac{\cancel{\beta}}{\cancel{\beta}}Q_m + \frac{c}{\cancel{\beta}}\frac{\cancel{dT}}{\cancel{dt}}$$

Integrating in the vicinity of the "bump".

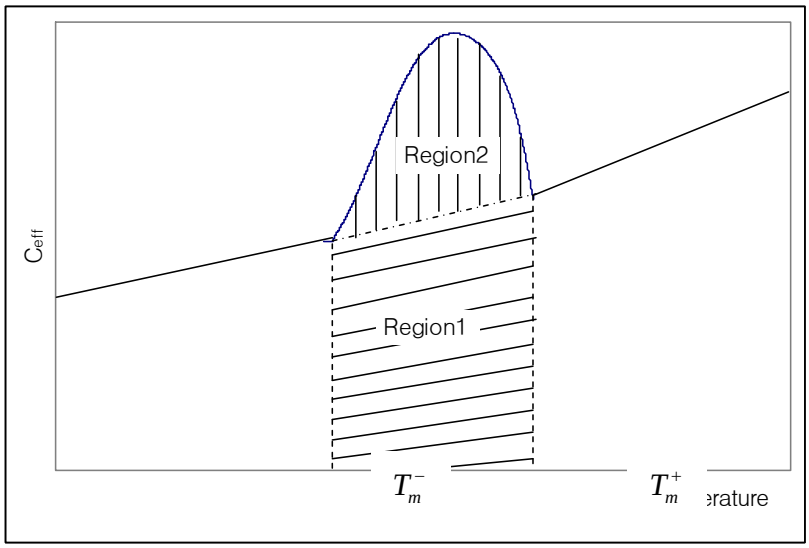

Figure 3-9. The effective specific heat

$$\int_{T_m^-}^{T_m^+} c_{eff}\,dT = \frac{1}{m}\int_{m_s}^{0}(-dm_s)Q_m + \int_{T_m^-}^{T_m^+} c\,dT$$

$$= Q_m + \int_{T_m^-}^{T_m^+} c\,dT$$

where the second term on the right is given by the area of Region 1, and Q_m is the area of the bump, Region 2. A similar process is used to determine the heat of decomposition.

From Equation (3-19c)

$$\int \frac{\dot{q}}{\beta m_i} dT = \int c_{eff}\, dT$$

$$= \frac{1}{m_i} \int_{m_i}^{m_f} \frac{(-dm)}{(1 - X_C)} Q_p + \int c dT$$

$$= Q_p + \int c dT$$

And Q_p is the area under the bump.

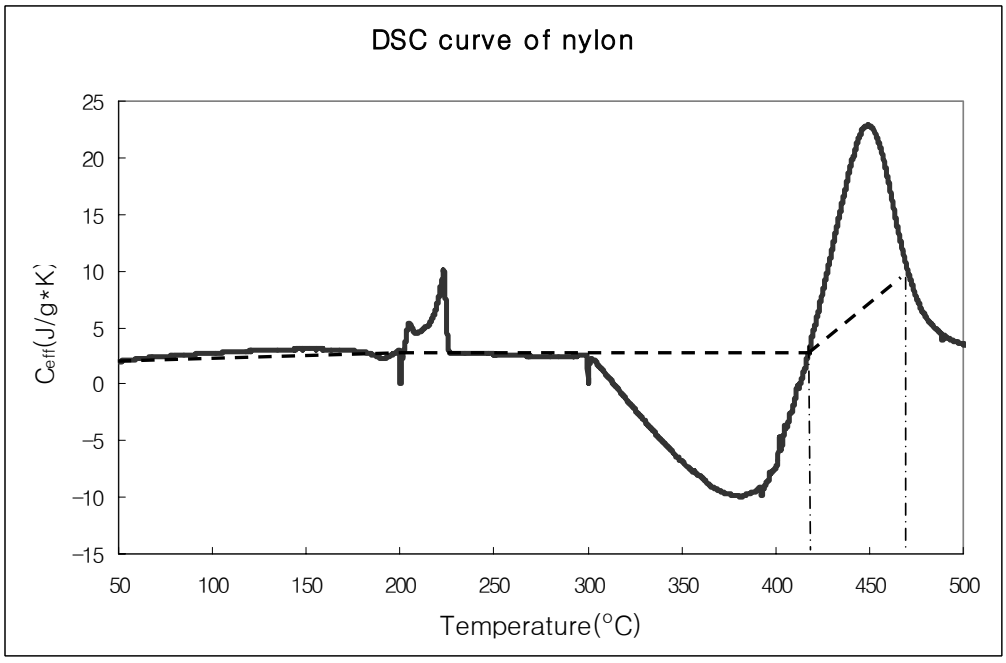

Figure 3-10. DSC signal of Nylon; estimating effective specific heat.

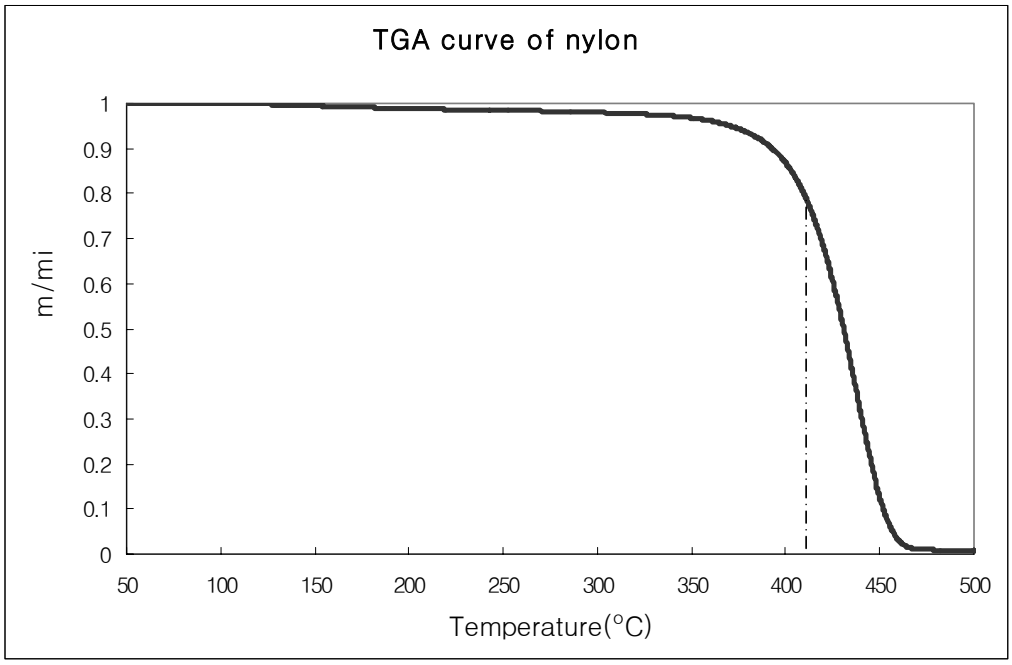

Figure 3-11. Comparing TGA signal to DSC signal of nylon; the temperature range in which decomposition occurs.

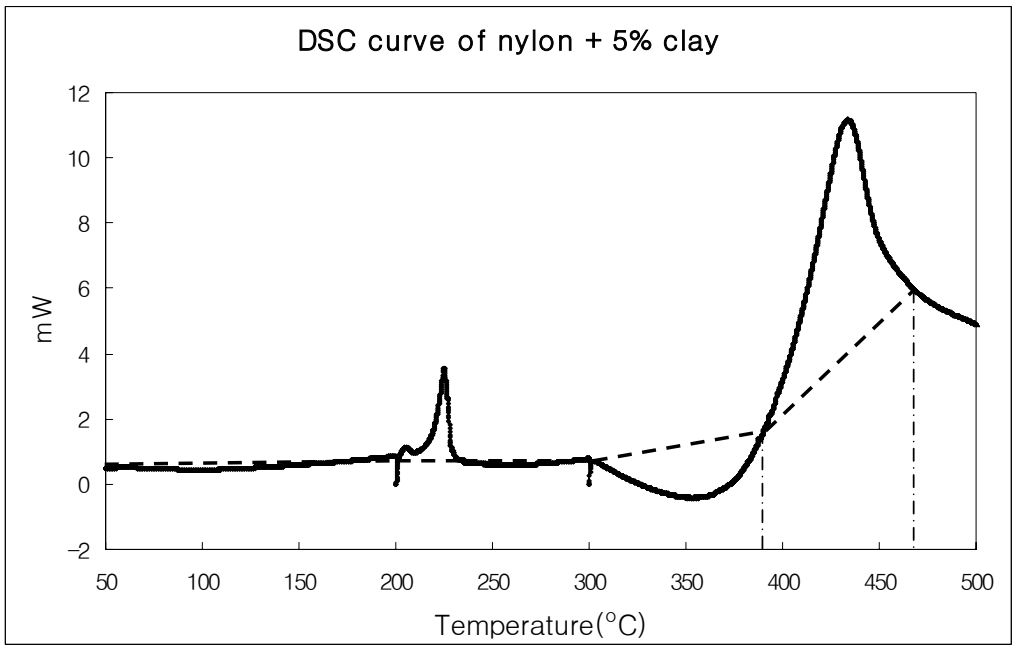

Figure 3-12. DSC signal of Nylon+5% clay; estimating effective specific heat.

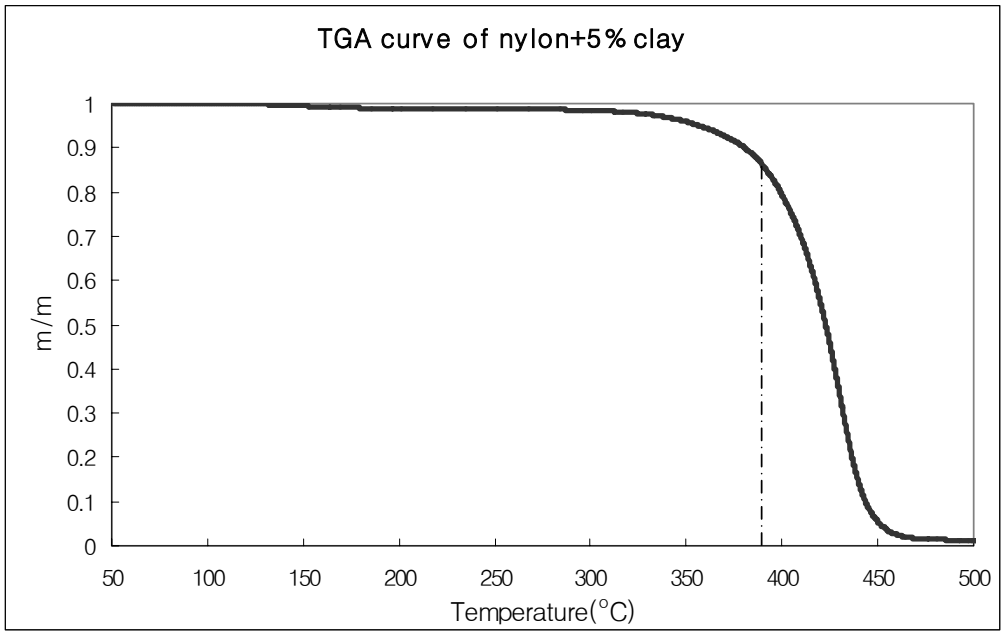

Figure 3-13. Comparing TGA signal to DSC signal of nylon+5% clay; the temperature range in which decomposition occurs.

Figures 3-10 and 3-11for nylon, and Figures 3-12 and 3-13 for nylon+5% clay display the temperature ranges in which decomposition occurs. For both material, DSC signals later than TGA.

As also shown in Figures 3-10 and 3-12, there are several bumps. First bump at lower temperature means melting and the area of bump is the heat of melting of Nylon and Nylon+5% clay, respectively. Likewise, second bump means decomposition and the area of bump is heat of decomposition of the both materials[14]. We conducted DSC experiments repeatedly, so the heat of decomposition ranges from 522 kJ/kg to 671 kJ/kg. It can be compared with the data from Chris Lautenbeger[8]. He showed 786 kJ/kg heat of decopmsition of nylon 6. Heat of melting from our data ranges from 32 kJ/kg to 73 kJ/kg. Ismat A. Abu-Isa reported the heat of melting of nylon 6 is 71 kJ/kg [15].

Table 3-1. Heat of decomposition of Nylon and nylon +5% clay

Nylon +5% clay	
Heating rate: 5℃/min	618kJ/kg, 671kJ/kg
Heating rate: 2℃/min	557kJ/kg
Heating rate: 10℃/min	522kJ/kg
Nylon	
Heating rate: 5℃/min	549kJ/kg, 388kJ/kg

Table3-2. Heat of melting of Nylon and nylon +5% clay

Nylon +5% clay	
Heating rate: 5℃/min	35kJ/kg, 73kJ/kg
Nylon	
Heating rate: 5℃/min	32kJ/kg, 35kJ/kg

Also, the dot line segments in Figures 3-10 and 3-12 give the specific heat over temperature in which sample undergoes heating, melting, and decomposition. That is, specific heat can be obtained by dividing the sample signal by the sample mass and heating rate. Specific heats of nylon and nylon with 5% clay are 1.5~3.4 J/g·K and

1.6~3.4 J/g·K respectively over the temperature range of roughly 50℃~300℃ in Figure 3-10 and 3-11. Kashiwagi[13] and Lautenberger[8] report that the specific heat of pure nylon ranges from about 1.5 J/g·K to 3.5J/g·K over temperatures of 25 ℃~250 ℃ and from about 1.5 J/g·K to 2.8 J/g·K over temperatures of 17 ℃~327 ℃ . Therefore, the DSC results analyzed are consistent with their values.

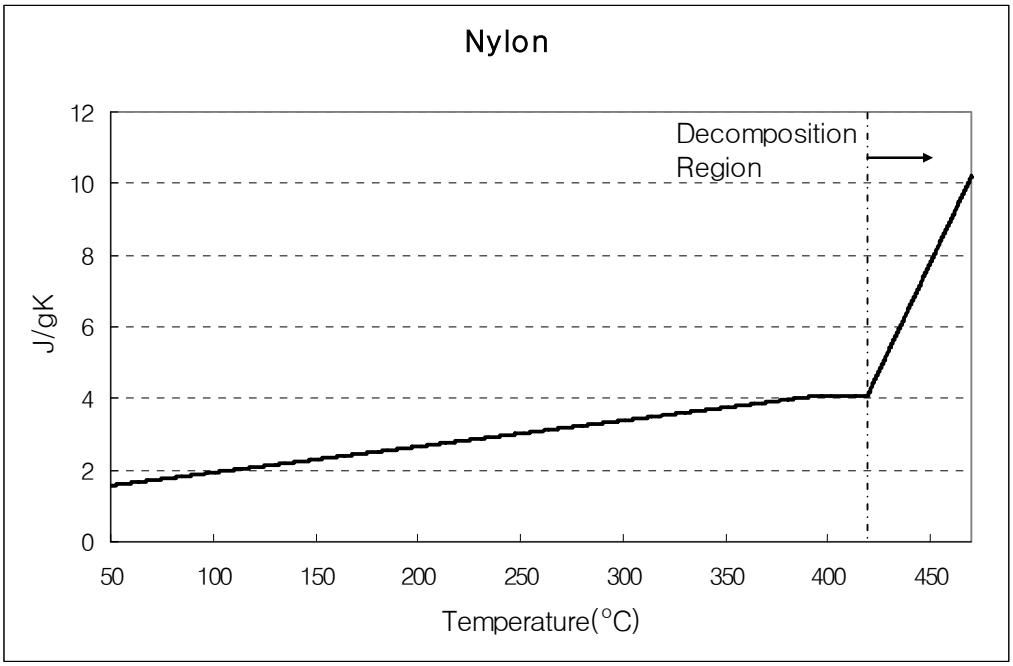

Figure 3-14. Specific heat of Nylon

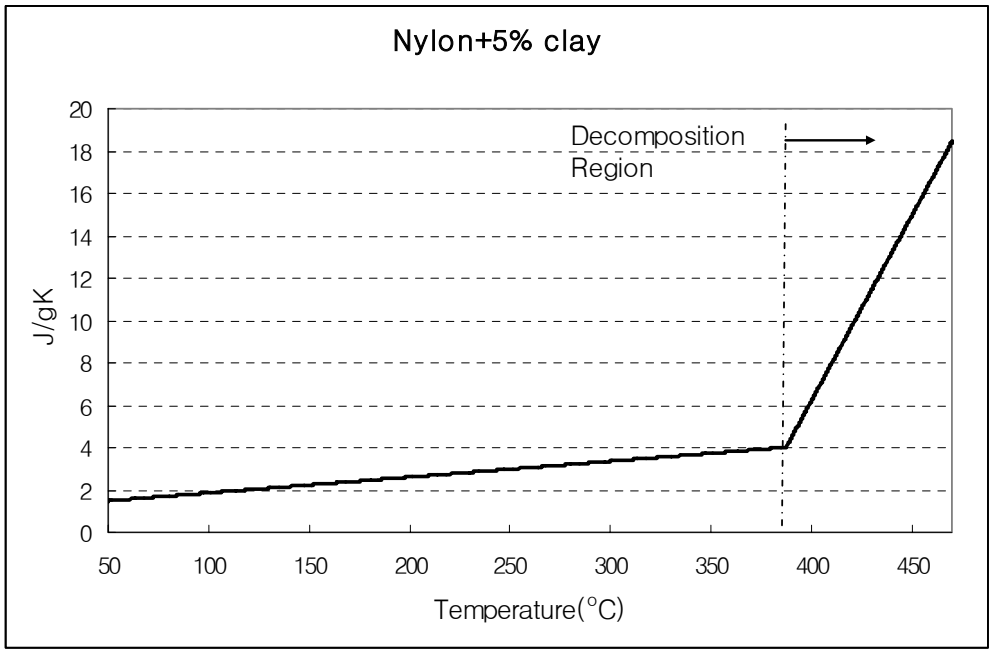

Figure 3-15. Specific heat of Nylon+5%

Here we need more discussion about the specific heat during decomposition. Before decomposition, the mass of sample is constant as the initial mass, and then after decomposition occurs, the mass decreases as vapor evolves. Figures 3-14 and 3-15 show the specific heat per unit initial mass for the whole periods, so the specific heat in the decomposition period is not the value for the charring mixture. Hence, we used TGA data to get the specific heat for this mixture.

From Equation (3-20)

$$c_{eff} = \frac{\dot{q}}{\beta m_i} = \frac{mc}{m_i}$$

where c is the specific heat of the mixture as follows.

$$mc = m_c c_c + m_a c_a \qquad (3\text{-}21)$$

From Equation (2-14) and

$$\frac{dm_c}{dt} = -X_C \frac{dm_a}{dt}$$

$$\int_0^{m_c} dm_c = -X_C \int_{m_i}^{m_a} dm_a$$

$$\frac{m_c}{m_i} = (1 - \frac{m_a}{m_i}) X_C$$

Then Equation (3-21) becomes

$$\frac{mc}{m_i} = \frac{m_c}{m_i} c_c + \frac{m_a}{m_i} c_a$$

$$= (1 - \frac{m_a}{m_i}) X_c c_c + \left(\frac{m/m_i - X_c}{1 - X_c} \right) c_a$$

$$= \left[1 - \left(\frac{m/m_i - X_c}{1 - X_c} \right) \right] X_c c_c + \left(\frac{m/m_i - X_c}{1 - X_c} \right) c_a \qquad (3\text{-}22)$$

Here, for nylon+5%, the specific heat at $m = m_i$ is 4 J/gK and that at $m = m_f$ is 18 J/gK during decomposition (Figure 3-15). The specific heat at $m = m_f$ can be calculated as follows

$$18 = \left(\frac{1 - X_c}{1 - X_c} \right) X_c c_c + 0$$

$$c_c = \frac{18}{X_C} = \frac{18}{0.05} = 360 J / g \cdot K$$

As seen, the value of 300 J/g·K is too high, and that of nylon, 625 J/g·K, is also too high. Consequently, though those values are theoretically right, it is far from the reality. When the burning rate of thermally thin material is modeled, the values of the asymptotic line is used as the specific heat in Figure 3-16 and 3-17. Therefore, the specific heat of nylon during decomposition is $c_p \left[\frac{kJ}{kg \cdot K} \right] = -78.876 + 0.2126(T - T_\infty)$, and that of nylon+5% clay is $c_p \left[\frac{kJ}{kg \cdot K} \right] = -82.119 + 0.2195(T - T_\infty)$. These values might be useful for the modeling.

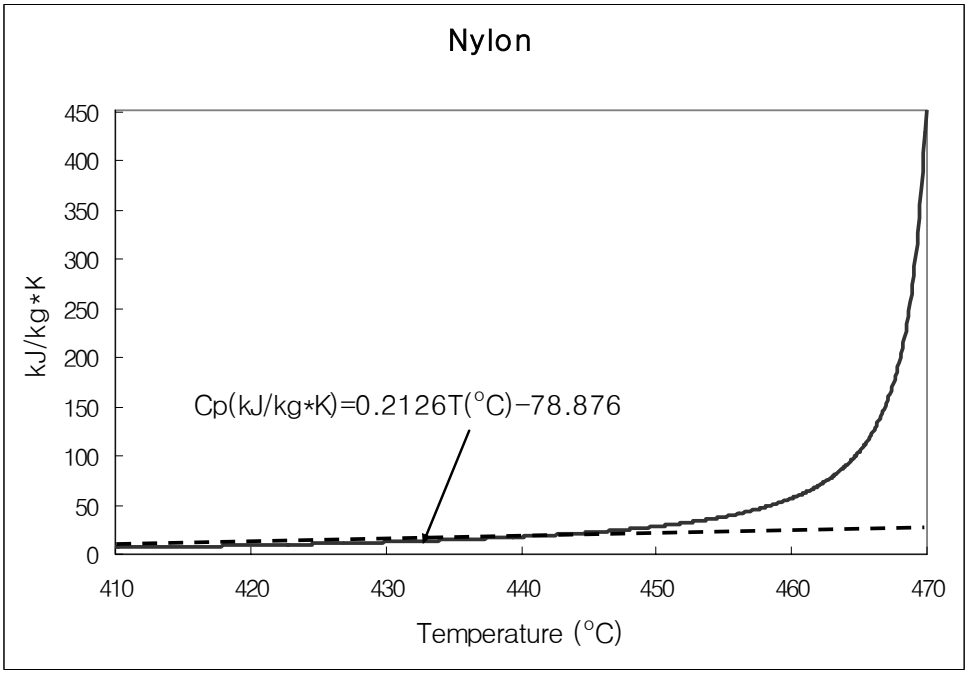

Figure 3-16. Specific heat of Nylon during decomposition

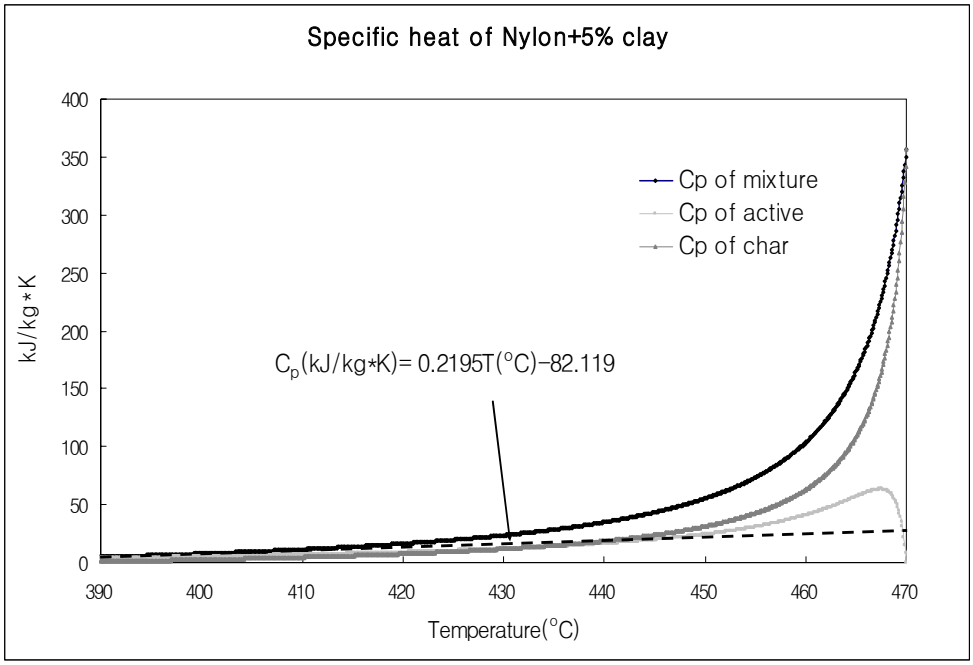

Figure 3-17. Specific heat of Nylon+5% during decomposition

Chapter 4: Modeling burning rate of thermally thin material

4-1. Introduction

It is desirable to have a means of determining the burning behavior of a material in terms of measurable properties. A general model for predicting the burning rate of materials is needed to accomplish this. Previous chapters showed the material goes through physical and chemical changes with specific kinetic and thermodynamic properties when the material is heated up. With the kinetic and thermodynamic properties from TGA/DSC, the burning rate of thin polymers under radiant heat can be formulated. The equations are solved by Mathematica.

The model results will be derived in terms of the derived TGA/DSC kinetic and thermodynamic properties instead of empirical the data from the cone calorimeter experiments carried out by Xin Liu[2, 16]. Previous measurements conducted under a cone calorimeter heating assembly for irradiances ranging from about 19 to 54kW/m^2 are used to check our model. A schematic layout of the apparatus is shown in Figure 4-1. The experimental procedure consisted of exposing a sample in the horizontal orientation to a constant external irradiance from the cone heater. The back side of the sample was insulated by 1inch thick Kaowool board (Type M) to minimize heat loss effects. In addition, an electrical arc igniter was applied approximately 1cm above the surface of the sample. The igniter was used as a pilot ignition source. These cone calorimeter experiment configurations will be applied to the modeling.

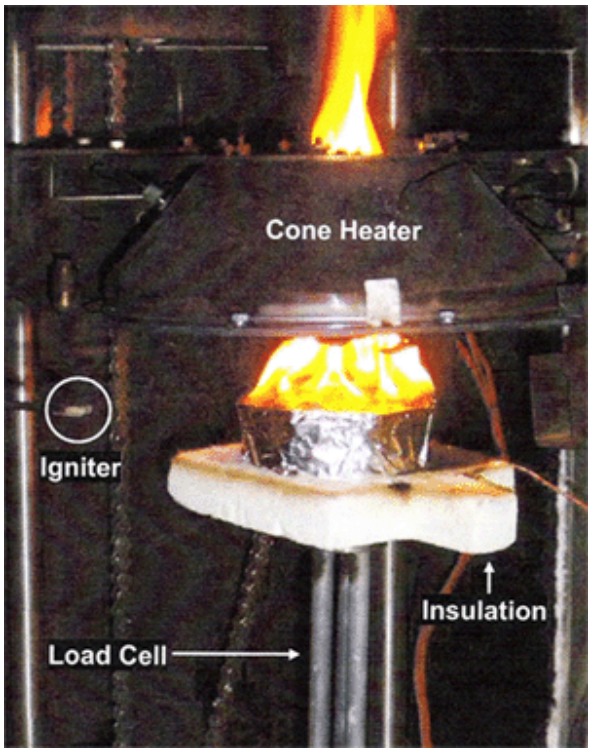

Figure 4-1.Cone calorimeter assembly

4-2. Theory

The model is formulated from the conservation laws. The transient exposure and response of the thin material is divided into 4 phases: (1) pre-heating to melt, (2) melting, (3) decomposing to ignition, and (4) flaming burning phase. Also, a thermally thin material dealt with in this study has no temperature gradient in itself. It means the temperature in the material would ideally be uniform throughout.

A control volume surrounding the thin sample is depicted in Figure 4-2. It shows the heating configuration for a material of thickness, δ . Let us consider the theory a condensed phase by a constant incident heat flux ($\dot{q}_i''$) from the cone heater, flame heat flux ($\dot{q}_f''$) after flaming burning, convective heating flux ($\dot{q}_c''$) when no flame is present,

reradiative heat flux ($\dot{q}''_{r,r}$) to a large surrounding at T_∞, and conductive heating flux ($\dot{q}''_b$) to the insulator on the bottom[17]. There is also gaseous fuel with enthalpy h_g leaving after decomposition occurs. The energy equation flows for a constant pressure system.

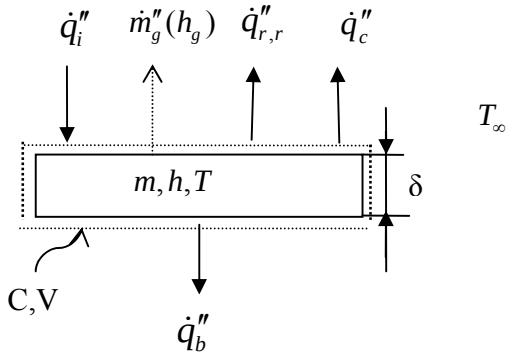

Figure 4-2. Heating of a material

The governing equation is

$$\rho c_p \delta \frac{dT}{dt} = \dot{q}'' + Q_m \frac{\rho\delta}{\triangle t_m} + Q_p \frac{d\rho}{dt}\delta \qquad (4\text{-}1)$$

where $\dot{q}''$ is the net heat flux which involves all of the heat fluxes mentioned above.

In the previous chapter DSC, the sample went through the melting and decomposing processes under heating, so the governing equation includes terms of melting and decomposing.

Q_m is the heat of melting. In the DSC chapter, it was determined 35kJ/mol for Nylon and 73kJ/mol for Nylon +5% clay added.

$\triangle t_m$ is the time period to melt.

Q_p is the heat of decomposition. In the DSC chapter, it was determined 550kJ/mol for Nylon and 670kJ/mol for Nylon +5% clay added.

The equations for each phase are outlined below:

4-2-1. Pre-heating to melt

In this phase, there is no chemical reaction such as melting and decomposition, but just heating up to the melting point. For Nylon and Nylon+5% clay, the pre-heating occurs in the range from 25℃ (298K) to 200℃ (473K), the melting point.

$$\rho c_P \delta \frac{dT}{dt} = \dot{q}'' = \dot{q}_i'' - \dot{q}_{r,r}'' - \dot{q}_c'' - \dot{q}_b'' \qquad (4\text{-}2)$$

$$\rho c_P \delta \frac{dT}{dt} = \alpha \dot{q}_i'' - \varepsilon\sigma(T^4 - T_\infty^4) - h_c(T - T_\infty) - \sqrt{\frac{\pi k' \rho' c_p'}{4t}}(T - T_\infty) \qquad (4\text{-}3)$$

where (1) ρ is the density of nylon and Nylon+5% clay, 1110kg/m^3 for both Nylon and Nylon+5% clay. For the density of Nylon and Nylo+5% clay, there is no difference between two due to the small amount of clay, and it is assumed that the volume of material does not change throughout the whole process of this modeling, even melting and decomposition process.

$c_p\left[\frac{kJ}{kg \cdot K}\right] = 1.1164 + 0.0075(T - T_\infty)$, specific heat of nylon

$c_p\left[\frac{kJ}{kg\cdot K}\right]=1.2067+0.0073(T-T_\infty)$, specific heat of nylon+5% clay

The specific heat changes linearly with temperature increasing, which comes from the DSC data analysis.

(2) $\dot{q}''_{r,r}=\varepsilon\sigma\left(T^4-T_\infty^4\right)$, reradiative heat flux

where $T=T(t)$, temperature of the sample

T_∞ is ambient temperature, 25℃.

δ is the thickness of sample

α is the absorptivity of the hot surface

ε is the emissivity of the hot surface

Assume the surface emissivity is equal to the absortivity as 1.

$\sigma=5.67\times10^{-11}kW/m^2\cdot K^4$, Stefan-Boltzmann constant

(3) $\dot{q}''_c=h_c(T-T_\infty)$, convective heat flux

where $h_c=1\times10^{-2}kW/m^2\cdot K$, convective heat transfer coefficient. The experiment conducted by Xin shows h_c ranges from 9×10^{-3} to $12\times10^{-3}kW/m^2\cdot K$ [2]

(4) $\dot{q}''_b=\sqrt{\frac{\pi k'\rho' c'_p}{4t}}(T-T_\infty)$, conductive heating flux as the back surface heat loss.

The 1 in. Kaowool insulator used is considered as thermally thick material. The properties of Kaowool such as k' and ρ' are given by a manufacturer. k' is the conductivity of the Kaowool. Based on the given values of k', it can be expressible as a function of temperature(K) as following.

$$k'\left[W/m^2 \cdot K\right] = 0.0002T(K) - 0.0487$$

ρ' is the density of the Kaowool, 272kg/m^3.

c_p' is the specific heat of the Kaowool, but it is not provided by the manufacturer. Hence, approximately the specific heat of a similar of type of material, gypsum board is used, 0.95 kJ/kgK given by Gypsum Association.

4-2-2. Melting Phase

In this melting phase, the temperature is constant at the melting point, 200℃ given by DSC analysis. Because of the phase changes from a solid to a liquid, heat supplied to the sample is used to melt. The time needed to melt the whole sample will be calculated using the following equation. From Equation (3-19b)

$$\rho c_p \delta \frac{dT}{dt} = \alpha \dot{q}_i'' - \varepsilon\sigma(T^4 - T_\infty^4) - h_c(T - T_\infty) - \sqrt{\frac{\pi k' \rho' c_p'}{4t}} - Q_m \frac{d\rho}{dt}\delta \quad (4\text{-}4)$$

Where $\rho = \frac{m_s}{V}$ is the mass of solid per unit volume of the control volume.

Here, LHS of Equation (4-4) is zero because of no temperature change, and the new term of the heat of melting is added. In order to estimate the time to melt, first the heat flux to

the insulator is ignored, and then the time for melting is obtained using the Equation (4-5). Equation (4-5) is obtained by integrating Equation (4-4). This estimated time is used to get a more accurate melting time in the next step.

$$\triangle t' = \frac{[\alpha \dot{q}_i'' - \varepsilon\sigma(T^4 - T_\infty^4) - h_c(T - T_\infty)]}{Q_m \rho \delta} \qquad (4\text{-}5)$$

Finally, the melting time period considering the heat flux to the insulator is calculated again.

$$\triangle t = \frac{[\alpha \dot{q}_i'' - \varepsilon\sigma(T^4 - T_\infty^4) - h_c(T - T_\infty) - \sqrt{\frac{\pi k' \rho' c_p'}{4\triangle t'}}]}{Q_m \rho \delta} \qquad (4\text{-}6)$$

where Q_m is the heat of melting. i.e.,35kJ/kg for nylon and 73 kJ/kg for nylon+5% clay.

k' is 0.0459 W/m^{2}K at 200℃.

The melting continues from the time(t_{473K}) at 200℃ (473K) to the time, $t_{473K} + \triangle t$.

4-2-3. Decomposing Phase

In this phase, the material is heated again and undergoes decomposition over a specific temperature range. In decomposition, the original material breaks up to vapor and char. This chemical reaction of the decomposition follows a single-step first-order Arrehnius reaction applied in the TGA analysis.

It is assumed there is no accumulation of vapor in char-melt matrix; that is, the fuel gas generated by the decomposition leaves instantly from the surface of the melt-char matrix.

Therefore, the mass of the control volume is the mass of both, original material and char, so the mass decreases as the decomposition is proceeding.

Energy conservation

$$\rho c_p \delta \frac{dT}{dt} = \alpha \dot{q}_i'' - \varepsilon\sigma(T^4 - T_\infty^4) - h_c(T - T_\infty) - \sqrt{\frac{\pi k' \rho' c_p'}{4t}}(T - T_\infty) + Q_p \frac{d\rho}{dt}\delta \quad (4\text{-}7)$$

Decomposition Kinetics is given by combining of Equations (2-2) and (2-9)

$$\frac{d\rho}{dt} = -\rho_a a_p \exp(-E_a / RT) \quad (4\text{-}8)$$

By mass conservation described in Equation (2-13)

$$\frac{d\rho}{dt} = (1 - X_C)\frac{d\rho_a}{dt} \quad (4\text{-}9)$$

where $\rho = \rho(t)$, the density of mixture of the original material and char

$\rho_a = \rho_a(t)$, the density of the original material

$c_p\left[\frac{kJ}{kg \cdot K}\right] = -82.119 + 0.2195(T - T_\infty)$, specific heat of nylon

$c_p\left[\frac{kJ}{kg \cdot K}\right] = -78.876 + 0.2126(T - T_\infty)$, specific heat of nylon+5% clay, the specific heat of mixture which comes from DSC analysis

$X_C = 0.016$ and 0.05 are the respective char fractions of Nylon and Nylon+5% clay.

$Q_p = 550kJ/kg$, decomposition heat of Nylon from DSC data

$Q_p = 670kJ/kg$, decomposition heat of Nylon+5% clay from DSC data

$E_a = 223kJ/mol-K$, as activation energy, the values are for both, Nylon and Nylon+5% clay from the DSC analysis.

$a_p = 1.5\times10^{14}\ s^{-1}$, pre-exponential factor of Nylon from the DSC analysis.

$a_p = 2.1\times10^{14}\ s^{-1}$, pre-exponential factor of Nylon+5% clay from the DSC analysis

4-2-4. Flaming burning

As the decomposition continues, the sample finally reaches a temperature of piloted ignition. This is first the so called “flash point”. Then later at a higher temperature, defined as the temperature on which a continuous flame is sustained on the sample surface, the “fire point” is achieved. Flashing occurs on the surface of the sample prior to sustained flaming. In all cases of this modeling, first, the ignition time is considered as the fire point at which flaming is sustained over the entire surface of the sample. Second, the ignition time is considered at the flash point. The flaming burning phase starts at the fire point and ends in burning out, so the flame heat flux is added to the energy balance.

Energy conservation

$$\rho c_P \delta \frac{dT}{dt} = \alpha \dot{q}_i'' + \dot{q}_f'' - \varepsilon\sigma(T^4 - T_\infty^4) - \sqrt{\frac{\pi k'\rho' c_p'}{4t}}(T - T_\infty) + Q_p \frac{d\rho}{dt}\delta \quad (4\text{-}10)$$

Kinetics decomposition

$$\frac{d\rho}{dt} = -\rho_a a_p \exp(-E_a / RT)$$

Mass conservation

$$\frac{d\rho}{dt} = (1 - X_C)\frac{d\rho_a}{dt}$$

The time to the flash point can be formed by computing mass flux at the lower flammable limit.

The lower flammable limit (LFL)[18] is

$$Y_F = \frac{c_p(T_{f,ad} - T_\infty)}{\triangle h_c} \quad (4\text{-}11)$$

The LFL mass flux is

$$\dot{m}_F'' = \left(\frac{h_c}{c_p}\right)(Y_F - Y_\infty) = \frac{h_c(T_{f,ad} - T_\infty)}{\triangle h_c} \approx 0.46 g/m^2\,\mathrm{s} \quad (4\text{-}12)$$

Where $T_{f,ad}$ =1300℃, the critical temperature for both ignition and extinction in air.

Y_∞ is zero. Also, this flash point is based on the criteria, $\dot{m}_F'' \triangle h_c = 13 kW/m^2$, suggested by Quintiere[19].

$\triangle h_c$ is the heat of combustion of nylon and nylon+5% clay, Xin reported the heat of combustion,27~29 kJ/g[2]. The heat of combustion, 27kJ/g is used in this modeling.

Therefore, mass flux at the flash point is 0.46g/m^{2}s.

Next, the fire point can be found using the criteria that the critical energy release rate per unit area is a unique constant at fire point of about 52kW/m^2[18]. The mass flux at the fire point can be computed by

$$\dot{m}'' = \frac{\dot{Q}''}{\triangle h_c} = \frac{50kW/m^2}{28kJ/g} \approx 1.79 g/m^2 \text{ s}$$

From this point at which the mass flux of vapor is 1.79g/m^{2}sec, the flame settles on the surface of the sample.

Hence the flame heat flux now needs to be determined. However, accurate methods to predict flame radiation in such fires are not currently available. Knowledge of the flame heat flux is crucial to any attempt at developing methods to predict the burning rate of real materials. The flame heat flux for samples in the cone calorimeter appears to be approximately constant for a given material due to the flame configuration like a cylindrical shape[20]. Figure 4-1 shows a photograph of the sample burning under the cone heater assembly. Note that the shape of the flame is tall and narrow. The significant flame radiation to the surface comes from the lower part of the flame only inches above the top of the cone. Therefore, the flame heat flux is assumed to be constant, the flame heat flux can be calculated by

$$\dot{m}'' = \left(\frac{1}{L}\right)\dot{q}_i'' + \frac{\left[\dot{q}_f'' - \varepsilon\delta(T_v^4 - T_\infty^4)\right]}{L} \qquad (4\text{-}13)$$

Subsequently, a plot of the mass loss rate data as a function of the external incident heat flux has utility in determining the flame heat flux. The intercept on the abscissa indicates the flame heat flux. The data of the mass loss rate corresponding to external heat flux are given from the cone calorimeter experiment[2].

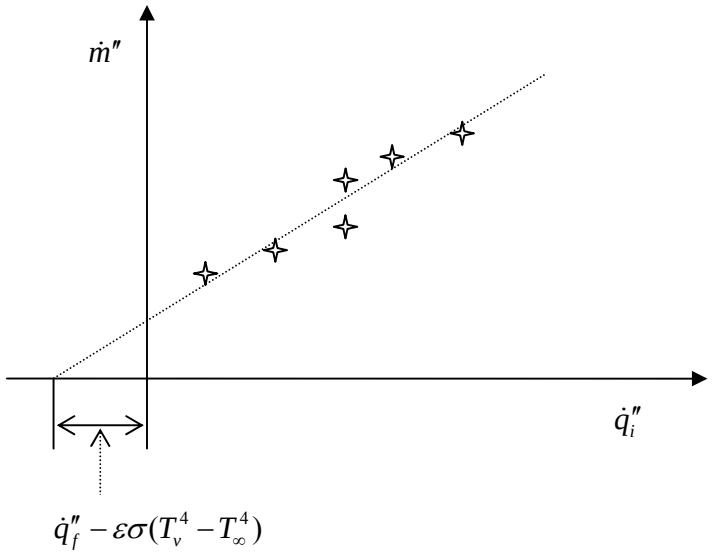

Figure 4-3. Determining flame heat flux using the plot of mass loss rate and external heat flux.

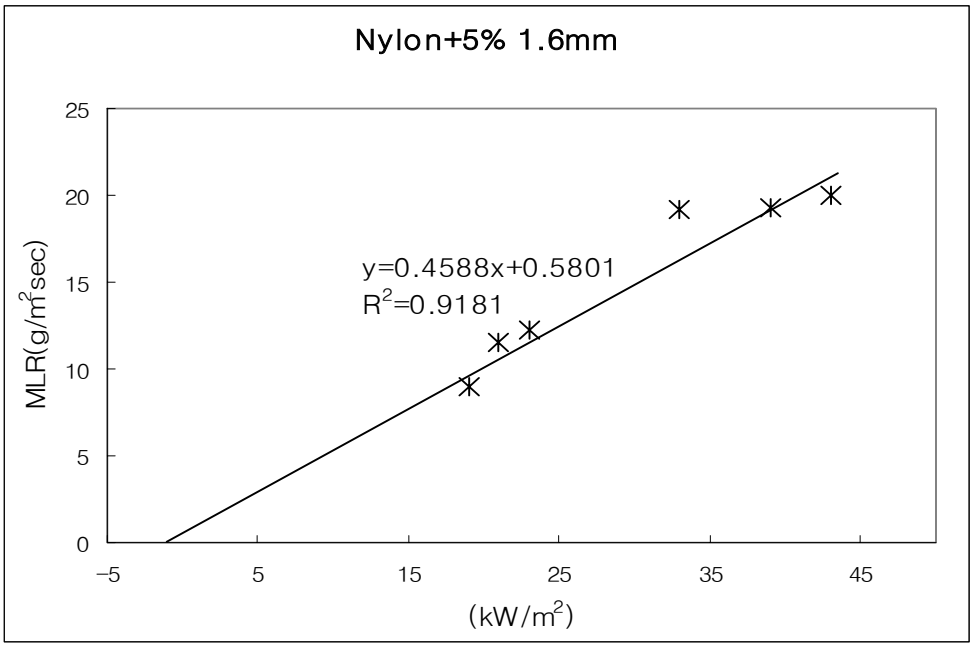

Figure 4-4. Determining flame heat flux for Nylon+5% 1.6mm.

The flame heat fluxes are shown in Table 4-1

Table 4-1. The flame heat flux in the Cone Calorimeter

	Nylon	Nylon+5% clay
1.6 mm	20 kW/m^2	20 kW/m^2
3.2 mm	30 kW/m^2	18 kW/m^2

Here, T_v is the surface temperature at which the mass loss rate of vapor is maximum. We have the option of initiating the flame at the flash point or the fire point. At the flash point, a premixed flame occurs and provides additional heat to the surface. Then if a diffusion flame is sustained, the fire point is achieved and now the heat from that flame is

felt. The flame heat flux that was estimated from the average peak burning rates is an average at this peak condition. That value is higher than at the onset of ignition. However, having no other reliable method to estimate the flame heat flux, this peak average value will be used as a constant from the onset of ignition. Both the flash and fire points will be investigated as the start of flaming.

Chapter 5. Results of modeling

5-1. Introduction

The model will be applied to data that exhibit thermally thin behavior. A criterion to classify the data as thermally thin will first be discussed. Then predicting for ignition and burning rate will be assessed. Thermally thin criteria can be considered in two cases. First, during the heating to ignition, the thermal wave could have the back-face of the sample at ignition. Subsequent heating would create a uniform temperature with the material for an insulated back-face. The material would have behaved as thermally thick for ignition, but now the burning is occurring with the sample fully heated at the start. Secondly, the sample could be thermally thick during most of the burning following ignition, but the thermal wave during burning eventually reaches the back-face. The depth of this thermal layer gives our indication of the magnitude of the decomposition zone. Figure 5-1 shows an example of burning 3.2mm thick nylon at different incident heat fluxes in the cone calorimeter. For high heat flux, steady burning is clearly indicated by the constant value achieved. However, following that steady value there is a sudden increase near the end of burning. This latter period of the burning occurs when the back-face begins heating. However, for the lowest flux, a thermally thin behavior is displayed during the whole burning.

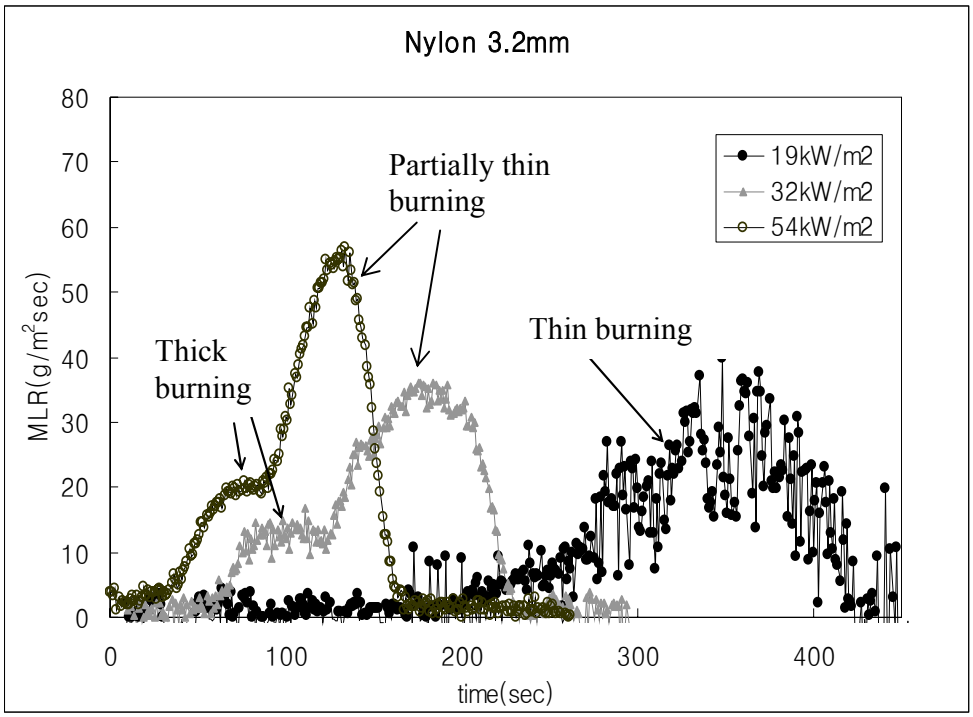

Figure 5-1. An example of thermally thick and thin burning behavior depending on the heat flux.

To obtain a criterion for thermally thin ignition, the study by Spearpoint and Quintiere[21] is examined. They report an approximate solution for ignition in terms of a thermal depth. The thermal depth varies as

$$\delta = \sqrt{3\left(\frac{k}{\rho c_p}\right)\left(\frac{2-\beta'}{1-\beta'}\right)t} \qquad (5\text{-}1)$$

where $\beta' = \dfrac{\sigma(T^4 - T_0^4) + h_c(T - T_0)}{\dot{q}_i''}$.

The time at ignition is given as

$$t_{ig} = \frac{4}{3} k \rho c_p \left(\frac{1-\beta'}{2-\beta'} \right) \frac{(T_{ig} - T_0)^2}{\dot{q}_i''^{\,2}} \tag{5-2}$$

Substitute this time into Equation (5-1). It shows the sample will ignite as thin material if $\delta(t_{ig}) \geq l$, then the criterion for burning as a thin sample is that the thickness, l, must be less than

$$l_{thin} = 2 \frac{(T_{ig} - T_0)k}{\dot{q}_i''} \tag{5-3a}$$

Here the incident heat flux is the external radiant flux. Also Staggs[11] obtains the thermal depth under steady burning as

$$\delta_s = \frac{2k(T_d - T_\infty)}{\dot{q}_{net}''} \tag{5-3b}$$

where T_d is the decomposition temperature and $\dot{q}_{net}''$ is the combination of incident flame and external radiative heat flux and reradiation, i,e., $\dot{q}_i'' + \dot{q}_f'' - \sigma(T_d^4 - T_\infty^4)$. Hence if the thickness of the sample, l, is less than δ_s, it will never achieve steady burning. Consequently, it will burn as thermally thin. The criteria is the same as Equation (5-3) for ignition except with the heat flux and surface temperature appropriately modified.

The burning behavior with the theory and the cone experimental data are examined. These results are described in Figures 5-2 and 5-3. The * designation signifies the thick burning behavior as illustrated in Figure 5-1, and the ▪ designated behavior as shown by the lowest flux level in Figure 5-1. The theoretical curves are based on Equation (5-3) using either the flash and fire points for the ignition temperature. Using Equation (5-3) with a higher net heat flux moves the theory closer to the data.

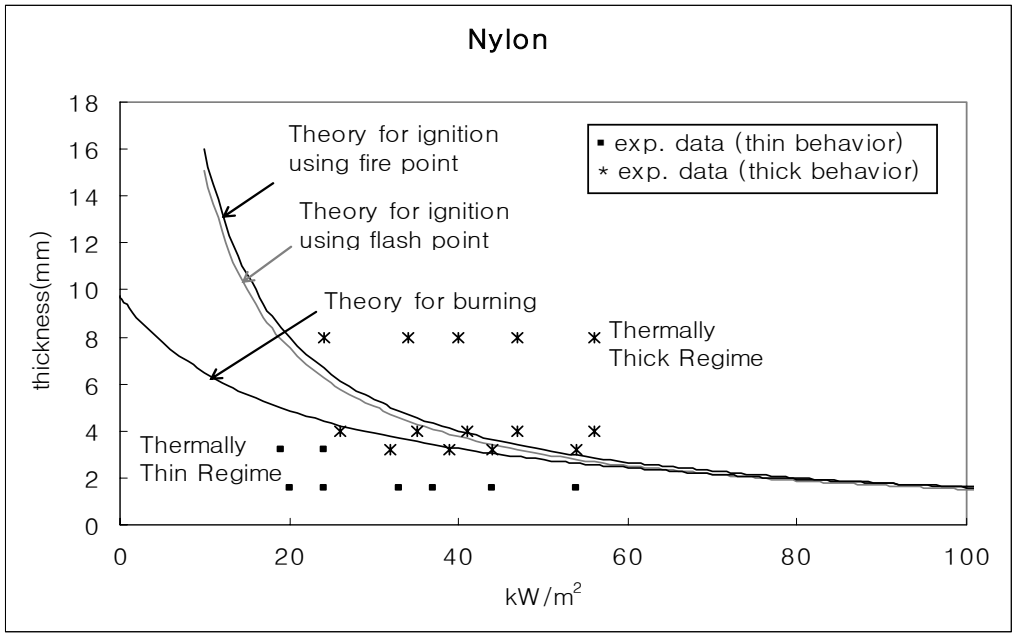

Figure 5-2. The burning behavior of Nylon with theory and the experimental data

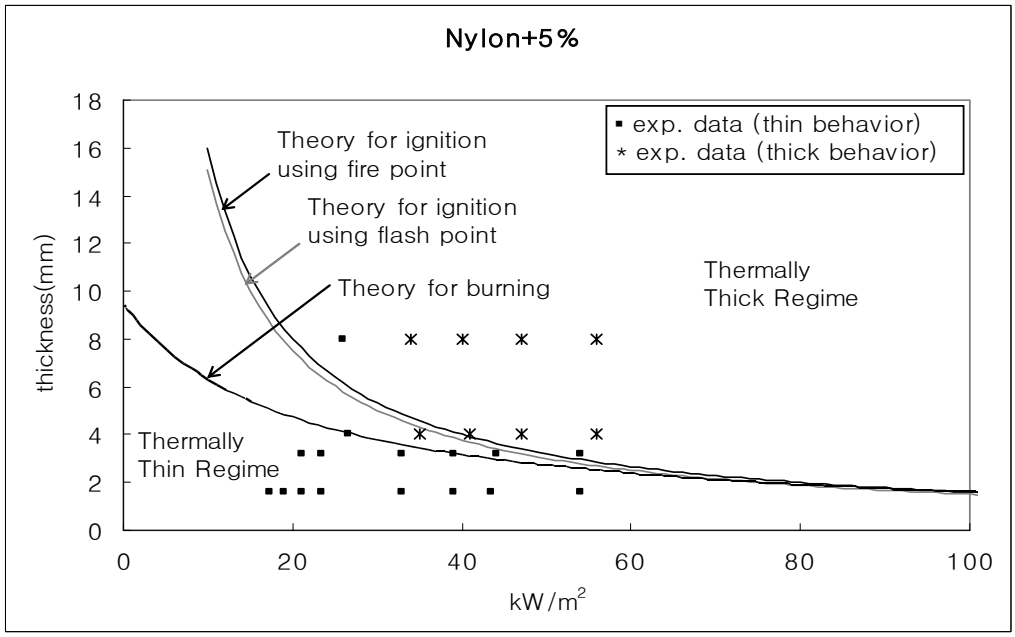

Figure 5-3. The burning behavior of Nylon+5% clay with the theory and the experimental data

As shown in Figures 5-2 and 5-3, the theory tends to follow the experimental data. Since our model was established on thermally thin theory, the simulation will only examine the cases in which materials burn as thermally thin in the cone calorimeter experiments. Thickness 1.6 and 3.2 mm are generally applicable to the theory.

5-2. Comparing the thermally thin burning model

5-2-1. Typical features of the model

Figure 5-4 shows the temperature change of 1.6mm nylon predicted by the model when the material is exposed to an external radiant heat flux of 20 kW/m^2.

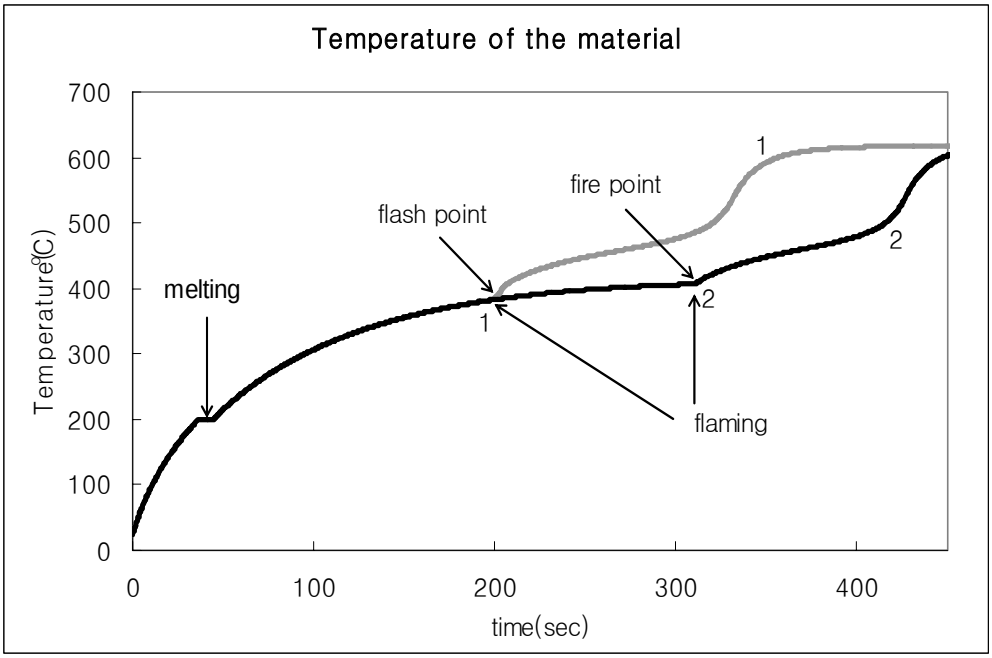

Figure 5-4. The temperature of Nylon with the thickness of 1.6mm under the incident heat flux, 20kW/m^2.

First, the material undergoes pre-heating. Second, melting occurs at 200℃, found by the TGA data. Third, the material starts to decompose, and then it reaches the flash point and fire point accordingly. Eventually, the material has flame on its surface, and so the burning rate accelerates. We considered both cases of a flame initiated at the flash point or fire point. Under low heat flux, it takes quite a long time to get the fire point after the flash point is achieved compared the case of high heat flux. Hence, the onset of burning significantly varies for these two ignition criteria under low heat flux. In contrast, the mass loss rate is almost the same in both cases as shown in Figures 5-5 and 5-6.

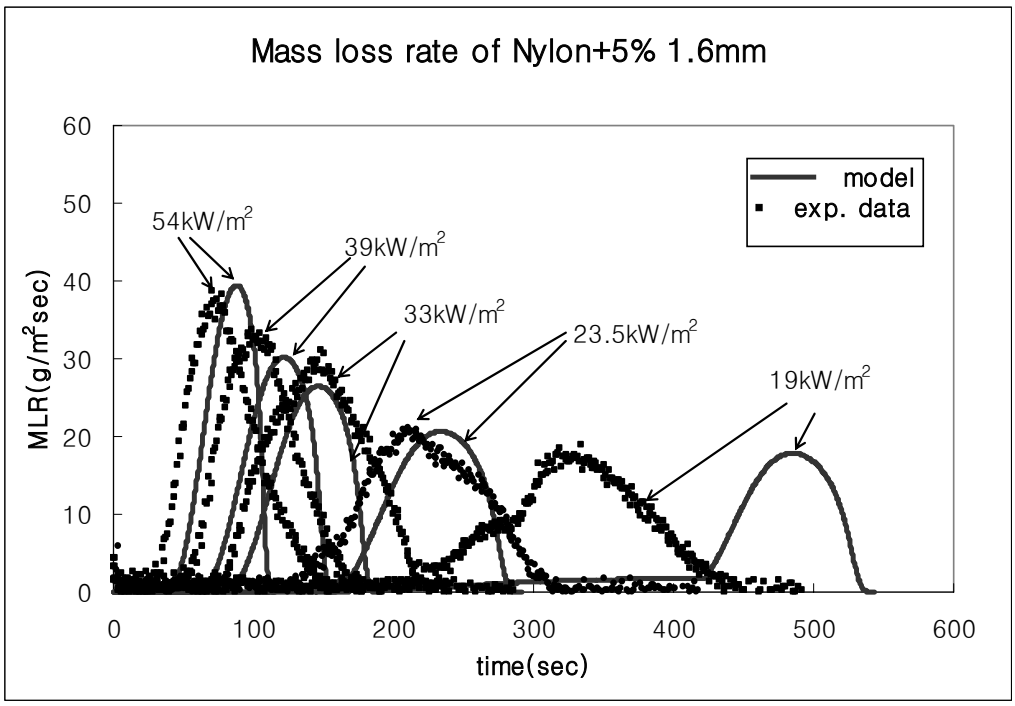

Figure 5-5. Comparing model with the cone calorimeter data: Flaming initiated at the fire point.

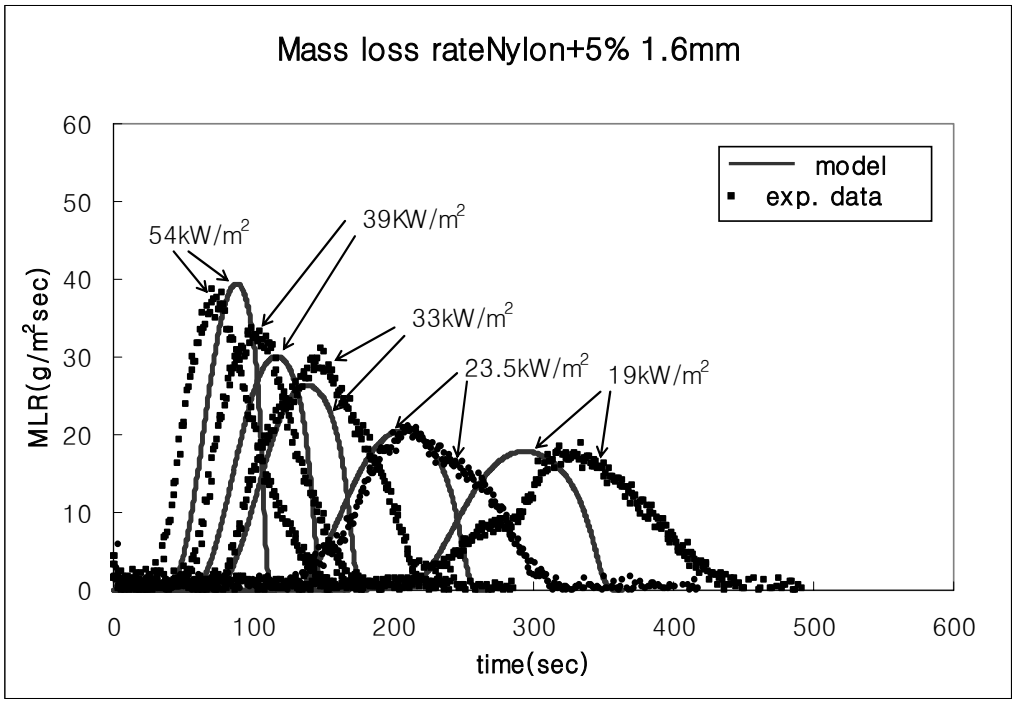

Figure 5-6. Comparing model with the cone calorimeter data: Flaming initiated at the flash point.

Figures 5-6 and 5-7 shows the accuracy of the model with the experiment. Also the variation in ignition time between the two flaming criteria can be seen. In general, in the case of nylon +5% with 3.2 mm thickness, the case in which a continuous flame is sustained on the material at the flash point has better agreement rather than the other case at the fire point. For instance, for the heat flux of 19kW/m^2, the ignition time of the model is very close to that of come calorimeter when the flame settles at the flash point. Other modeling results for 1.6mm thick and 3.2mm thick nylon, and 3.2mm thick nylon +5% clay are presented in Appendix A.

5-2-2. Ignition time

The theoretical ignition time is defined as the time at which the material reaches the fire point and flash point; namely, the fire point is when the mass loss rate is 1.79 g/m^{2}sec and the flash point is when the mass loss rate is 0.46 g/m^{2}sec (See chapter 4). As seen in Figures 5-7 and 5-9 for 1.6mm thick nylon and nylon+5% clay, ignition times in the experiment occur between the flash point and fire point of the model. In Figures 5-8 and 5-10, for 3.2mm thick nylon and nylon+5% clay, ignition times of the experiment occur faster than those predicted.

We now consider the critical heat flux for the ignition. The critical heat flux for ignition is defined when $t_{ig} \to \infty$. From the model, the critical heat fluxes for flash point and fire point are calculated as 16 kW/m^2 ~18 kW/m^2 and 19 kW/m^2 ~20 kW/m^2 for nylon and nylon+5% clay, respectively. Xin[2] reported that the critical heat flux for ignition is about 18~19 kW/m^2 as found in the experiments. The thermally thin model is not perfect for thickness as indicated by Figure 5-2.

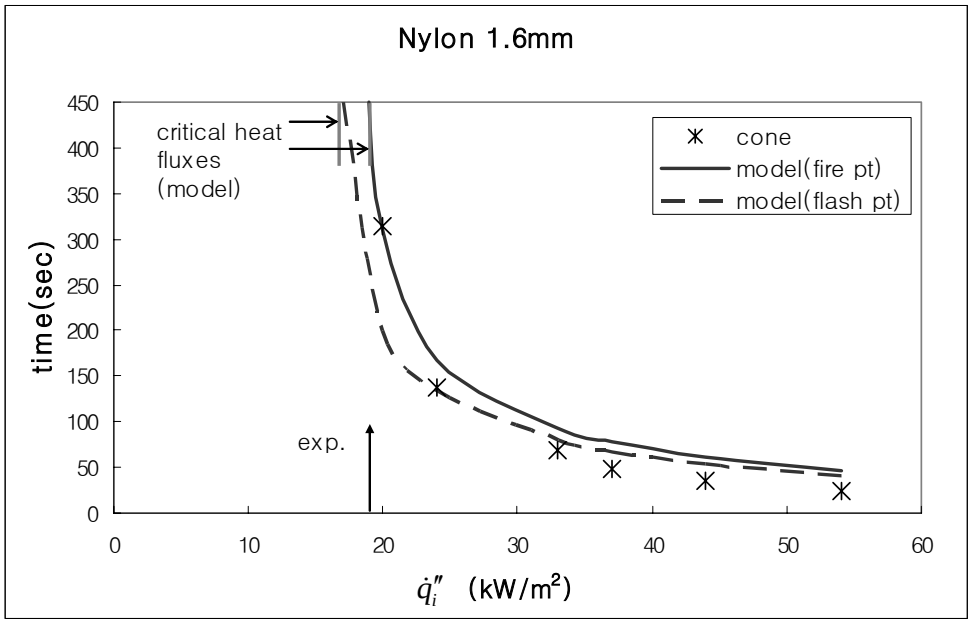

Figure 5-7. Ignition time of 1.6mm thick nylon from the cone exp. and the model using both flash and fire point.

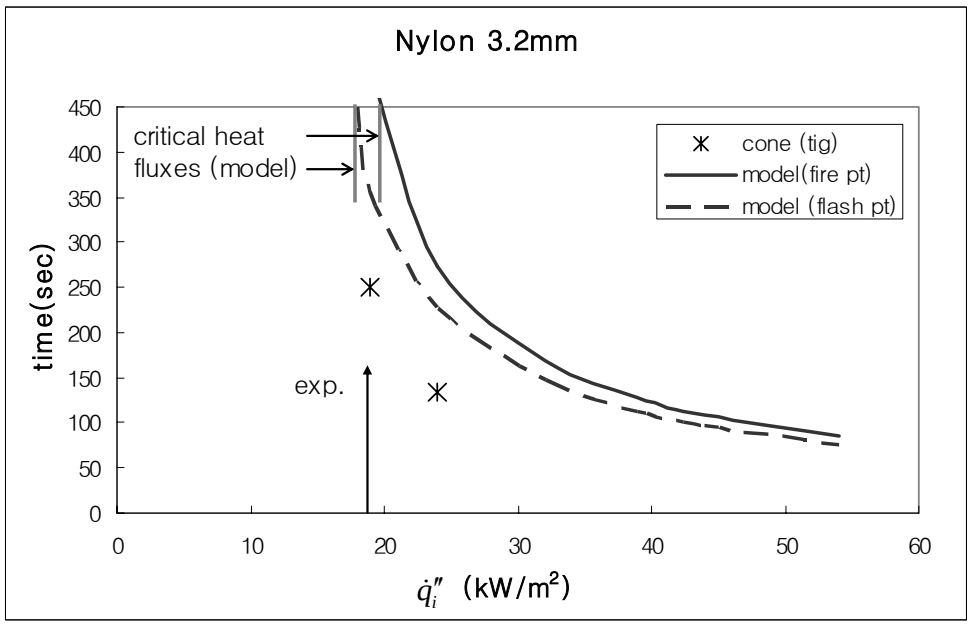

Figure 5-8. Ignition time of 3.2mm thick nylon from the cone exp. and the model using both flash and fire point.

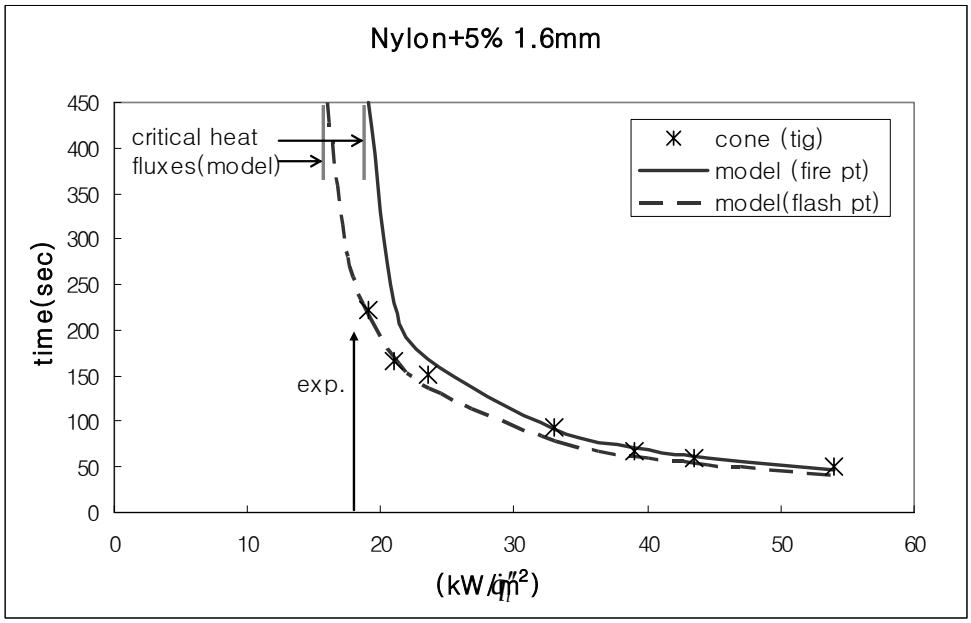

Figure 5-9. Ignition time of 1.6mm thick nylon+5% from the cone exp. and the model using both flash and fire point.

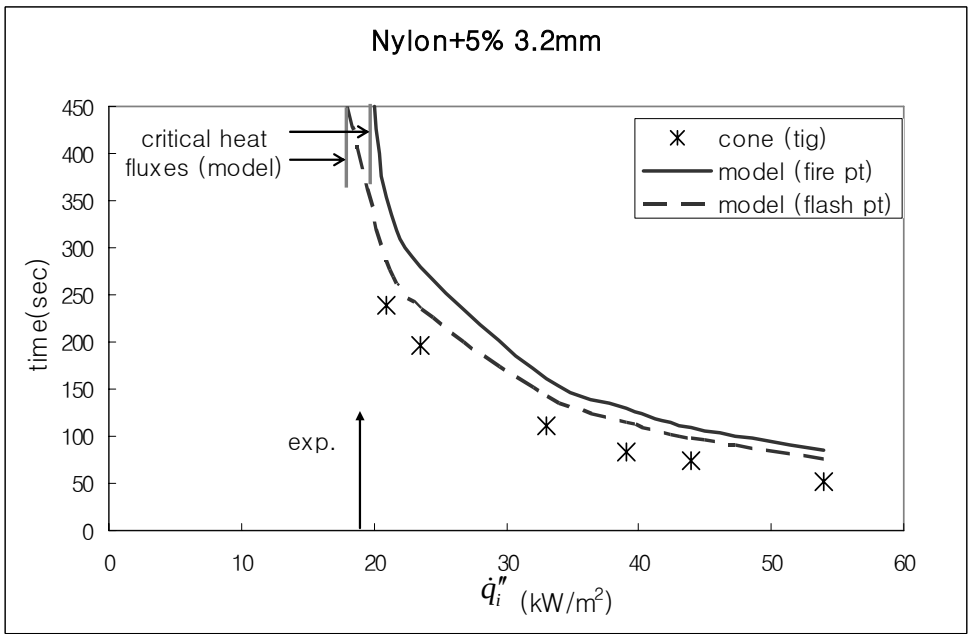

Figure 5-10. Ignition time of 3.2 mm thick nylon+5% clay from the cone exp. and the model using both flash and fire point.

5-2-3. Burning rate

After the flaming occurs, the burning rate increases quickly because of the increased heat flux from the flame. To compare the burning rate, the peak mass loss rate during the burning was identified. These results are shown in Figures 5-10, 5-11, and 5-12. For 1.6mm thickness of nylon and nylon+5% clay, the burning rate of the model coincides with that of the experiment. Comparatively, for nylon +5% clay at 3.2 mm thickness, the predictions exceed the data.

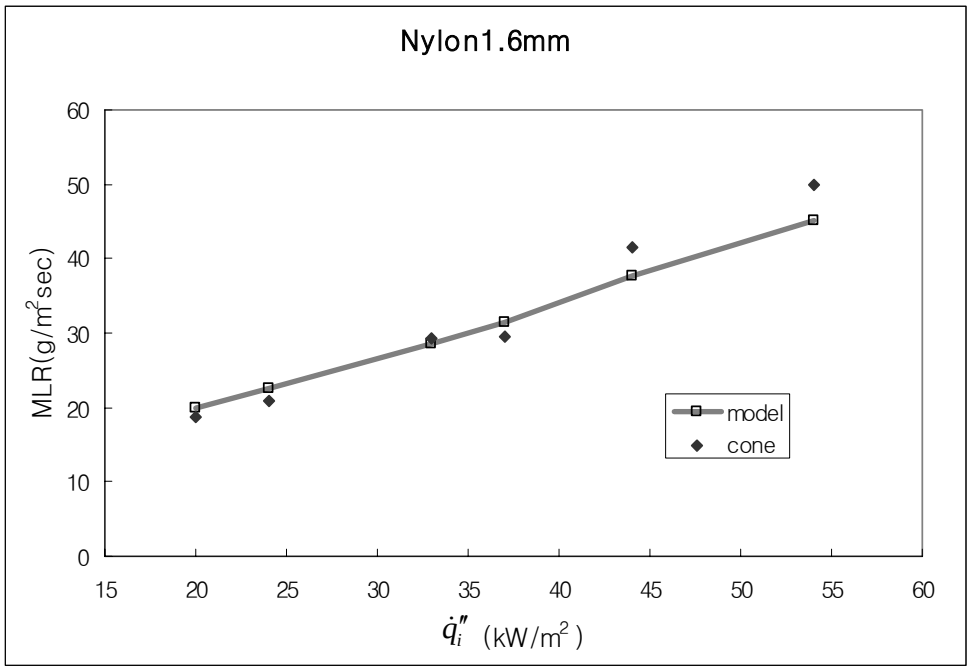

Figure 5-11. Mass loss rate of 1.6mm thick nylon.

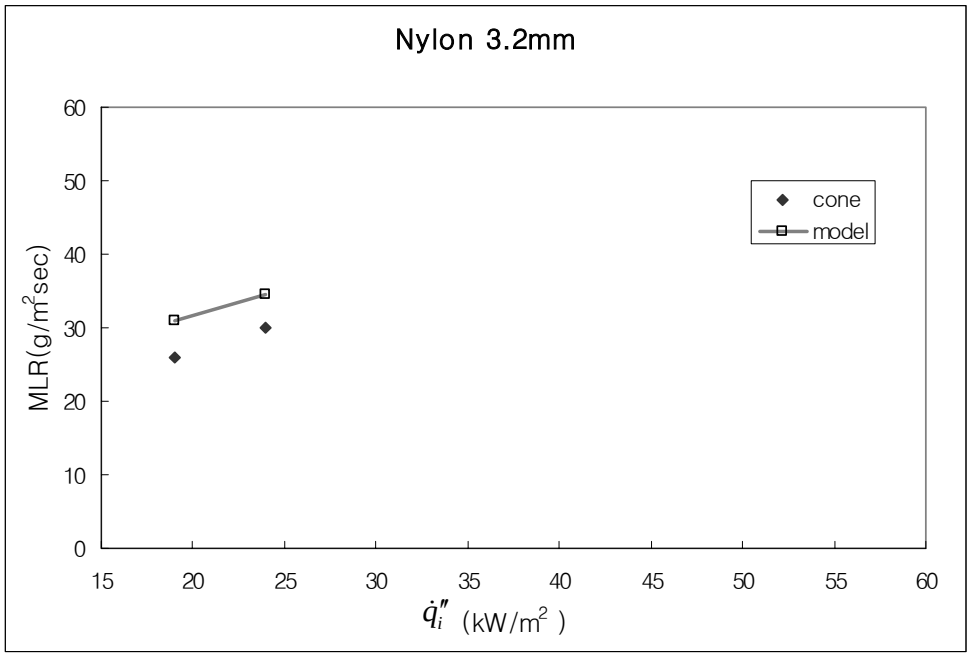

Figure 5-12. Mass loss rate of 3.2 mm thick nylon.

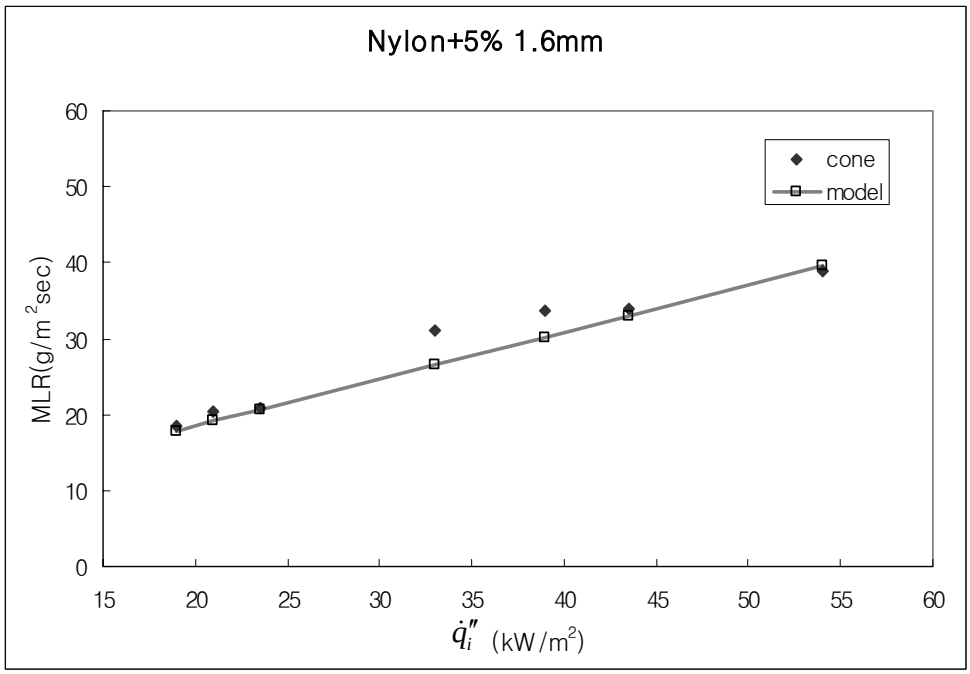

Figure 5-13. Mass loss rate of 1.6mm thick nylon+5% clay.

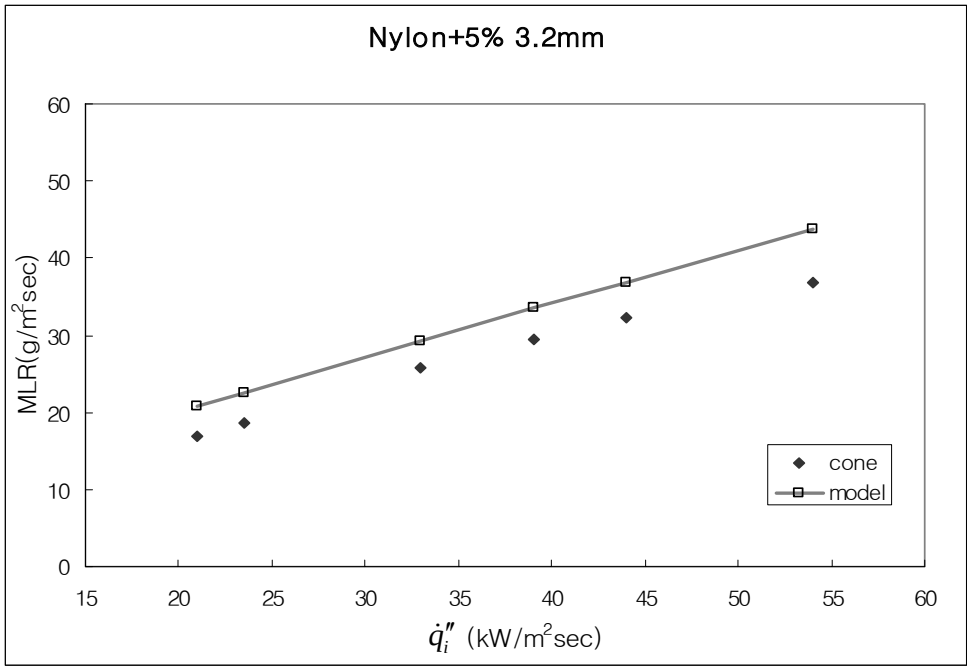

Figure 5-14. Mass loss rate of 3.2mm thick nylon+5% clay.

5-3. Other thermal properties

5-3-1. Flash point, fire point, and the temperature at the peak burning rate

The flash point and fire point calculated by the model are found to be constant over the heat flux range, but they do vary with the thickness and the composition.

Table 5-1. Computed flash points and fire points

	Nylon 1.6mm	Nylon 3.2mm	Nylon+5% clay 1.6mm	Nylon+5% clay 3.2mm
Flash point	383 ℃	372 ℃	378 ℃	367 ℃
Fire point	406 ℃	394 ℃	403 ℃	388 ℃

In contrast, the decomposition temperature varies. The temperature(T_p) at the peak burning rate increases with heat flux. These results are shown in Figure 5-13.

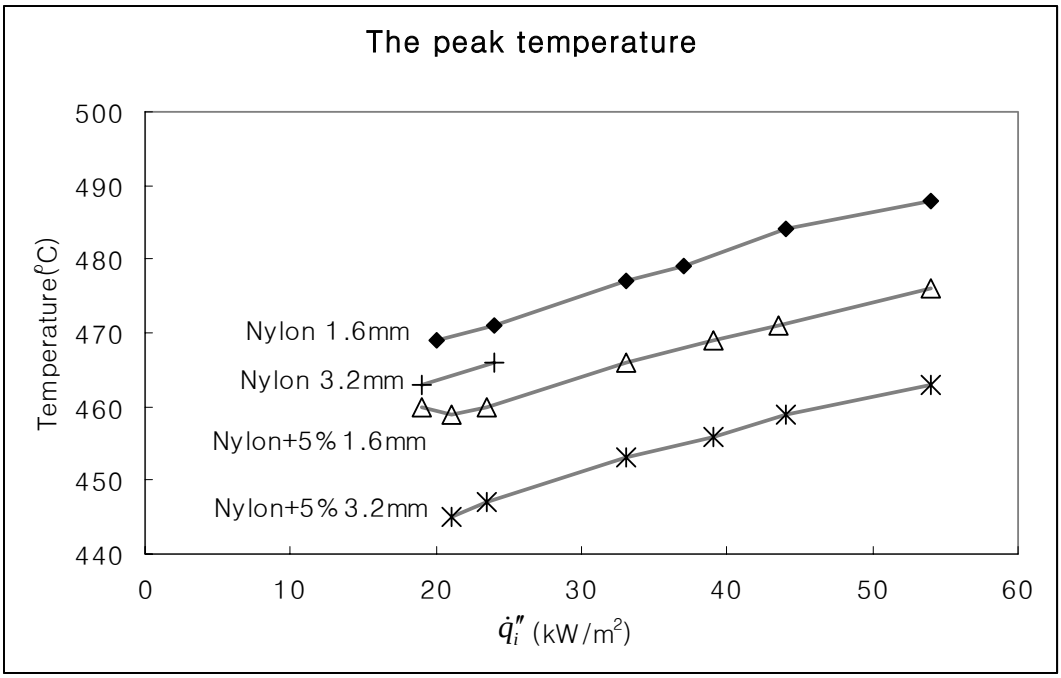

Figure 5-15. Decomposition temperature at the peak burning rate.

5-3-2. Gasification heat

The heat of gasification is the energy required during steady burning to vaporize the material. The heat of gasification, L [17], for the materials can be calculated by

$$L = \int_{T_o}^{T_m} c_{p,s} dT + Q_m + \int_{T_{liq}}^{T_d} c_{p,l} dT + Q_p$$

where 1) $\int_{T_o}^{T_{liq}} c_{p,s} dT$: the energy needed to raise a unit mass of solid from its original temperature T_o (25 ℃) to the melting point, T_m (200 ℃).

For nylon, $c_{p,s}\left[\frac{kJ}{kg\cdot K}\right]=1.1164+0.0075(T-T_{\infty})$ for the temperature range, from 25℃ to 200 ℃

For nylon+5% clay, $c_{p,s}\left[\frac{kJ}{kg\cdot K}\right]=1.2067+0.0073(T-T_{\infty})$

2) $\int_{T_m}^{T_p} c_{p,l}dT$: the energy needed to raise a unit mass of liquid from the melting point, T_m (200 ℃), to the decomposition temperature point, T_p [22] .

T_p is 450 ℃ for nylon, and 435 ℃ for Nylon+5% clay.

For nylon, in the range of temperature, from 200℃ to 410 ℃,

$$c_{p,s}\left[\frac{kJ}{kg\cdot K}\right]=1.1164+0.0075(T-T_{\infty})$$

and in the temperature range, from 410℃ to 450 ℃,

$$c_{p}\left[\frac{kJ}{kg\cdot K}\right]=-82.119+0.2195(T-T_{\infty})$$

For nylon+5% clay, in the range of temperature, from 200℃ to 390 ℃,

$$c_{p,s}\left[\frac{kJ}{kg\cdot K}\right]=1.2067+0.0073(T-T_{\infty})$$

and in the temperature range, from 390℃ to 435 ℃,

$$c_p\left[\frac{kJ}{kg\cdot K}\right] = -78.876 + 0.2126(T - T_\infty) \text{ from 390℃ to 435 ℃.}$$

3) Q_m : the heat of melting, 35 kJ/kg for nylon and 73kJ/kg for Nylon+5% .

Q_p : the heat of decomposition, 550 kJ/kg for nylon and 670kJ/kg for Nylon+5% clay.

These values such as $c_{p,s}$, $c_{p,l}$, T_m, T_p, Q_m, and Q_p came from the DSC analysis performed before. By computation, the heat of gasification for nylon and Nylon+5% clay are 2.14 kJ/g and 2.13 kJ/g, respectively. Here, we need to consider the char effect. We had the different char fraction for nylon and Nylon+5% clay, so the gasification heat should be modified as follows[17].

$$L_m = \frac{L}{1 - X_C} \qquad (5\text{-}4)$$

For Nylon, the gasification heat is 2.17 kJ/g, and for Nylon+5% clay, that is 2.25 kJ/g. In SFPE handbook[23], the gasification heat of Nylon 66 is 2.4 kJ/g, and in FAA report[22], that of Nylon 66 is 2.1 kJ/g.

5-3-3. Heating rates

The material on this study was exposed to various heating rates in the TGA and DSC apparatuses. The heating rates employed were 1, 2, 5, 10 ℃/min whereas the heating rates in the cone calorimeter experiments are relatively high. They are similar to real fire conditions. Hence, comparing these heating rates applied to the material is meaningful. The heating rate in the cone calorimeter was calculated as in Chapter 4.

1) Pre-heating phase (from 25 ℃ to the melting point, 200 ℃)

$$\rho \frac{dT}{dt} = \left[\alpha \dot{q}_i'' - \varepsilon\sigma(T^4 - T_\infty^4) - h_c(T - T_\infty) - \sqrt{\frac{\pi k' \rho' c_p'}{4t}}(T - T_\infty) \right] c_p \delta$$

2) Melting phase (at the melting point)

$$\frac{dT}{dt} = 0 \text{ for } \Delta t = \frac{[\alpha \dot{q}_i'' - \varepsilon\sigma(T^4 - T_\infty^4) - h_c(T - T_\infty) - \sqrt{\frac{\pi k' \rho' c_p'}{4\Delta t'}}]}{Q_m \rho \delta}$$

3) Decomposing phase (from the melting point to the fire point)

$$\frac{dT}{dt} = \left[\alpha \dot{q}_i'' - \varepsilon\sigma(T^4 - T_\infty^4) - h_c(T - T_\infty) - \sqrt{\frac{\pi k' \rho' c_p'}{4t}}(T - T_\infty) + Q_p \frac{d\rho}{dt} \delta \right] \rho c_p \delta$$

4) Flaming phase (from the fire point to burning out)

$$\frac{dT}{dt} = \left[\alpha \dot{q}_i'' + \dot{q}_f'' - \varepsilon\sigma(T^4 - T_\infty^4) - \sqrt{\frac{\pi k' \rho' c_p'}{4t}}(T - T_\infty) + Q_p \frac{d\rho}{dt} \delta \right] \rho c_p \delta$$

Figure 5-14 shows the difference in the heating rate between the external incident heat fluxes of 20, 39, 60 kW/m^2 in the cone calorimeter and the heating rate of 10 ℃/min in the TGA.

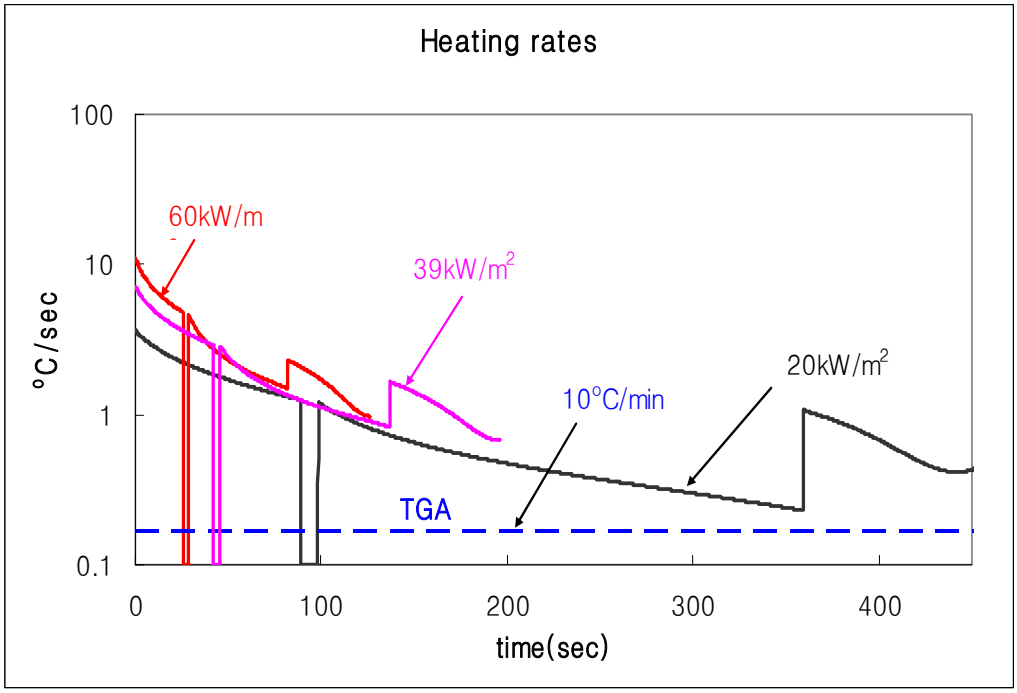

Figure 5-16. The heating rates in the TGA, DSC, and cone calorimeter.

Chapter 6. Conclusions

A first order reaction model was used to describe the kinetics of decomposition. Based on the first order, the Arrhenius parameters were obtained. Then, the kinetic model with the parameters was compared with the TGA data in Figures 2-10 and 2-11. At the heating rate, 5℃/min, the model is the best fit with the data. In sum, the model using a first order for decomposition reaction accords well with the experimental data.

The chemical kinetic and thermodynamic properties derived from the TGA and DSC data in chapters 2 and 3 were used to establish the model. The properties are in Table 6-1 and Table 6-2.

Table 6-1. Decomposition parameters used in the model.

	Activation Enegy (E_a)	Pre-exponential factor (a_p)	Heat of melting (Q_m)	Heat of decom. (Q_p)
Nylon	223kJ/mol*K	$1.5*10^{14}sec^{-1}$	35 kJ/kg	550 kJ/kg
Nylon+5%	223kJ/mol*K	$2.1*10^{14}sec^{-1}$	73 kJ/kg	670 kJ/kg

Table 6-2. The specific heats of nylon and nylon+5% clay over temperature used in the model.

Nylon	$1.116 + 0.0075(T - T_\infty)$ [kJ/kgK] from 25℃ to 410℃	$-78.9 + 0.213(T - T_\infty)$ [kJ/kgK] from 410℃ to 470℃
Nylon +5%	$1.207 + 0.0073(T - T_\infty)$ [kJ/kgK] from 25℃ to 390℃	$-82.2 + 0.220(T - T_\infty)$ [kJ/kgK] from 390℃ to 470℃

The temperatures, 410℃ and 390℃ are the onset temperature of the decomposition for the materials, and 470℃ is the temperature at the end of decomposition. These were given by DSC data.

Compared to the Cone Calorimeter data, the model in predicting thermally thin burning gives good agreement. Especially, modeling results for1.6mm thick nylon and nylon+5% compare well with the experimental data of burning rate and ignition time. The ignition time from the Cone Calorimeter occurs between the flash point and the fire point of the model. However, 3.2 thick samples showed some differences between the model and the experimental data; that is, the mass loss rate of the model is higher than that of the experiment, and the ignition in the model occurs later than that in the experiment. This means that the samples with the thickness of 3.2 mm are not perfect thermally thin.

Two different kinds of materials by composition were used. Flame retardant properties of clay nano-composites have been reported in many studies. The present model also displays the retardant properties. Burning rate of nylon with 5% clay is consistently lower than that of nylon under the same range of external radiation. In addition, the heat of melting, the heat of decomposition, and the heat of gasification for nylon +5% clay are

higher those for nylon. Consequently, the model with the experimental data together accounts reasonably for the flame retardancy of clay nano-composites.

APPENDIX. Modeling data compared the Cone Calorimeter Experiment

1. Nylon with 1.6mm

1) Flaming initiated at the fire point.

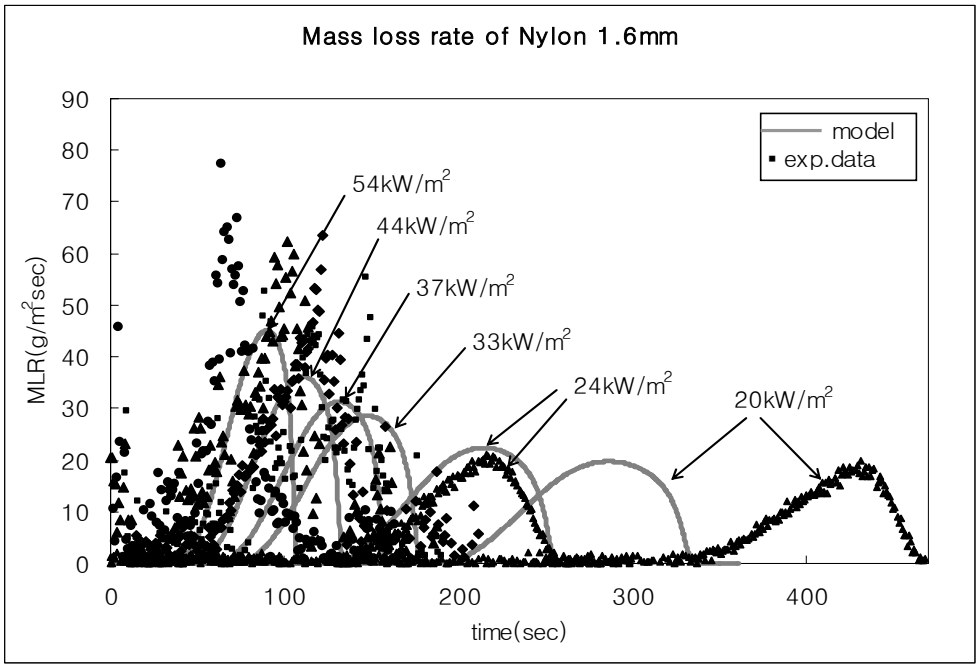

2) Flaming initiated at the flash point.

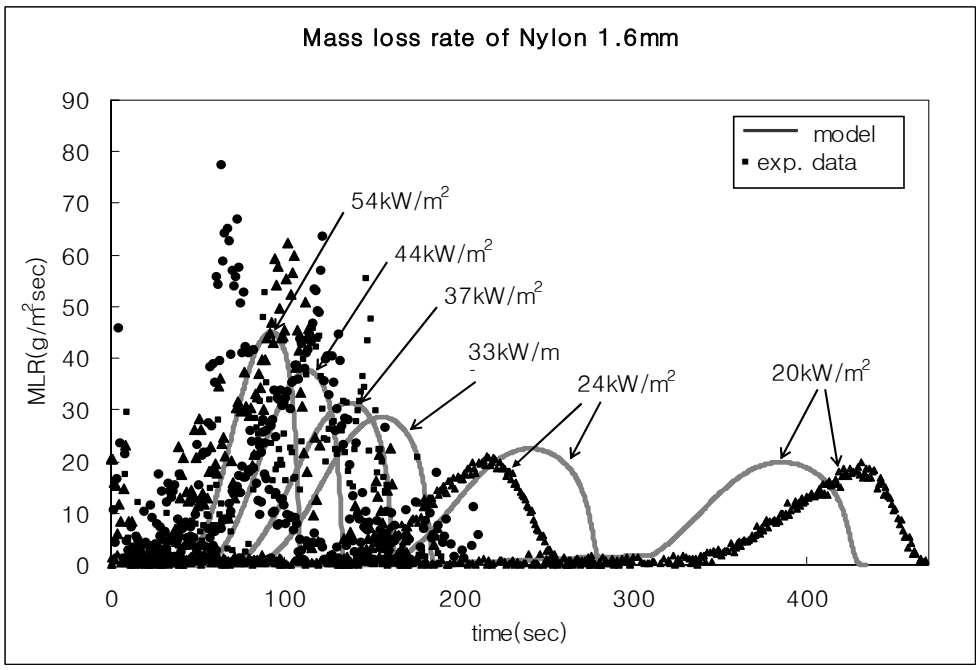

3) Flaming initiated at the flash point.

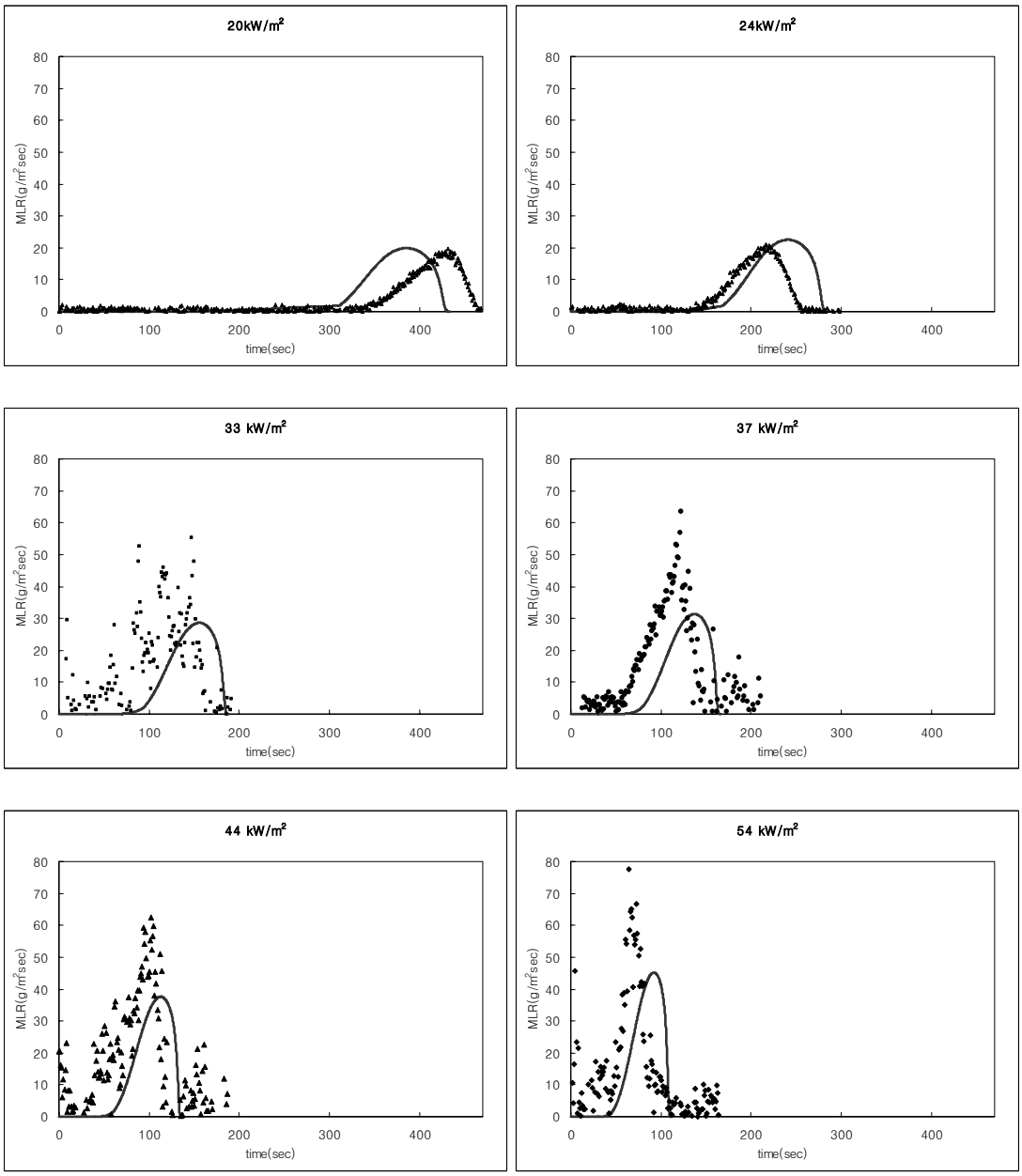

2. Nylon with 3.2mm

1) Flaming initiated at the fire point.

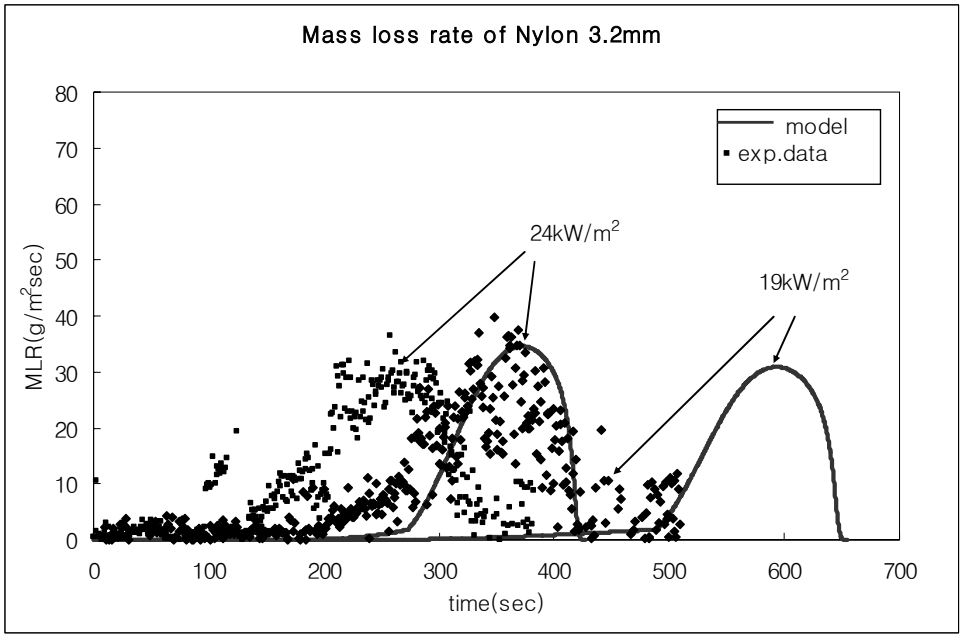

2) Flaming initiated at the flash point.

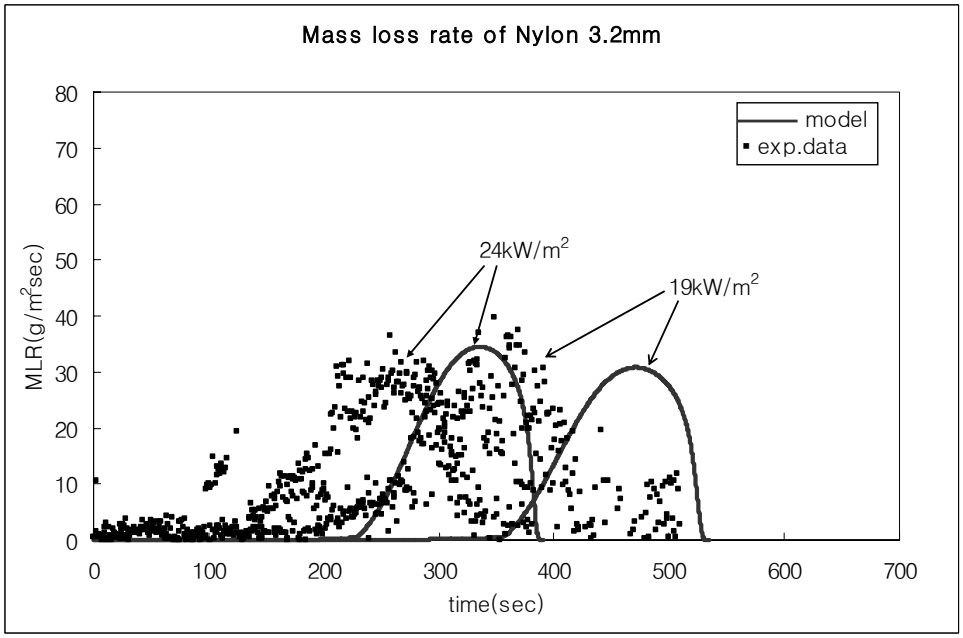

3) Flaming initiated at the flash point.

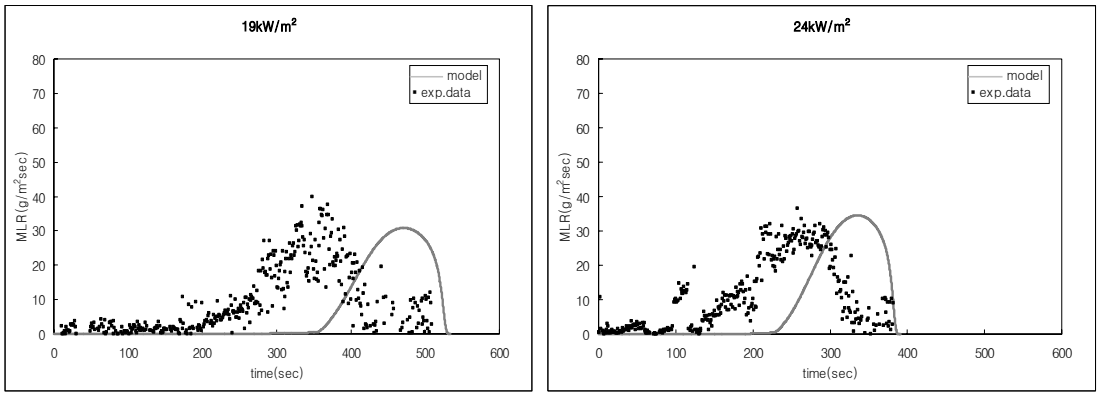

3. Nylon +5% clay with 1.6mm

1) Flaming initiated at the fire point.

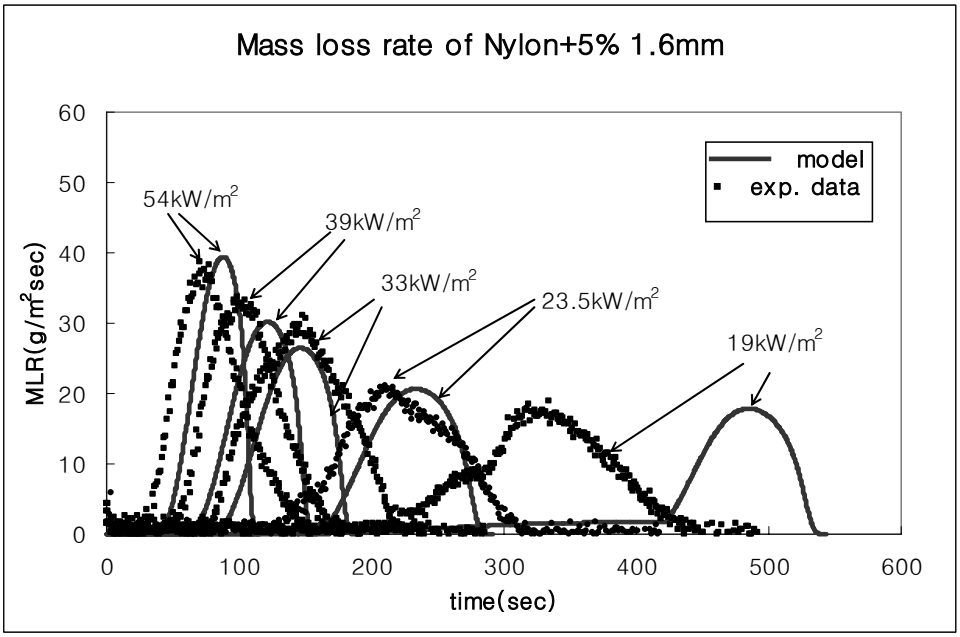

2) Flaming initiated at the flash point.

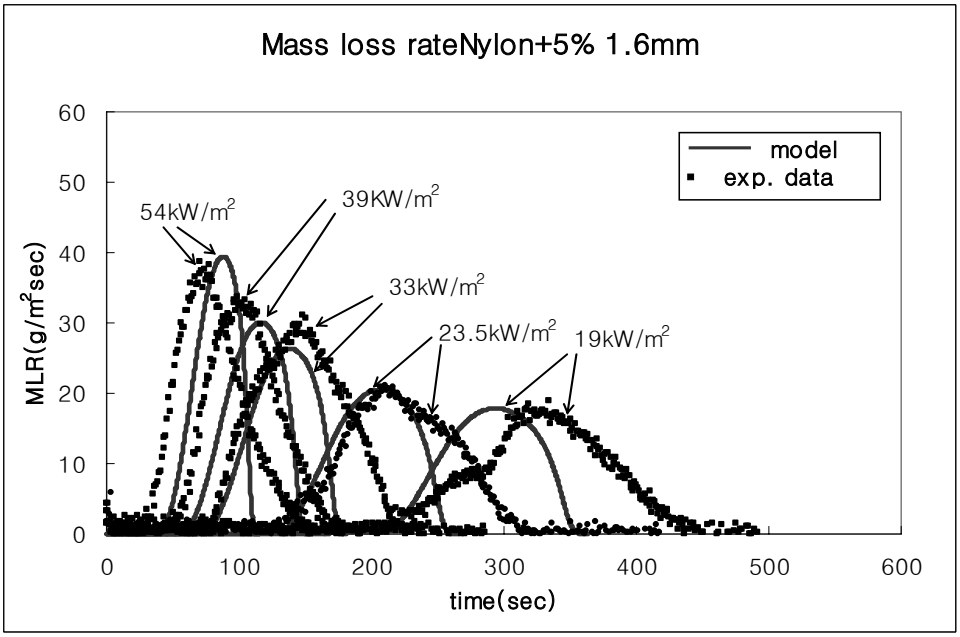

3) Flaming initiated at the flash point.

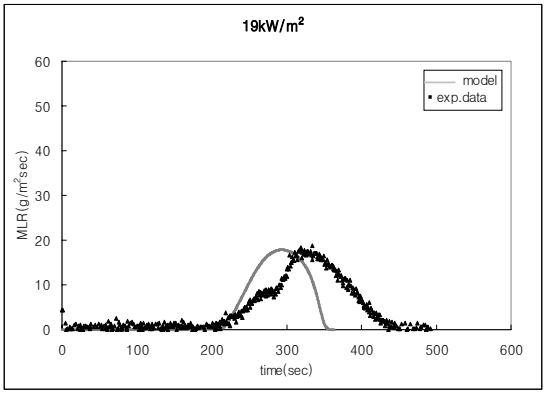

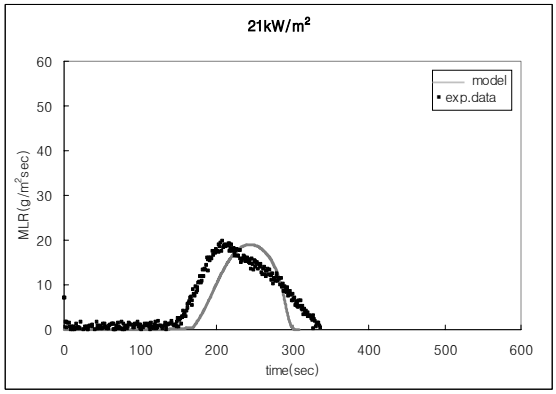

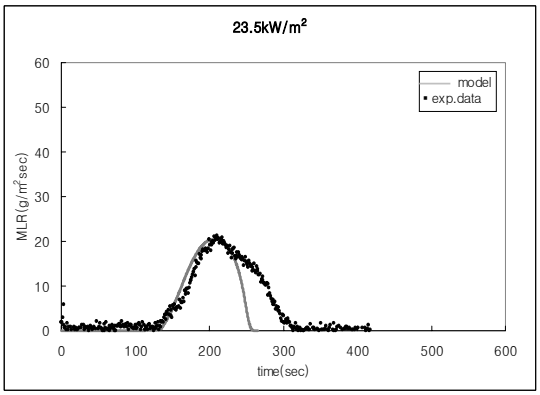

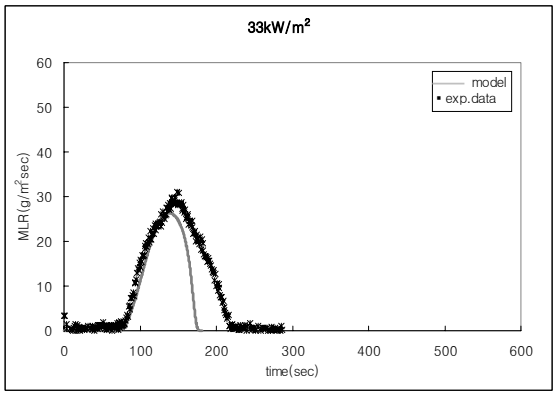

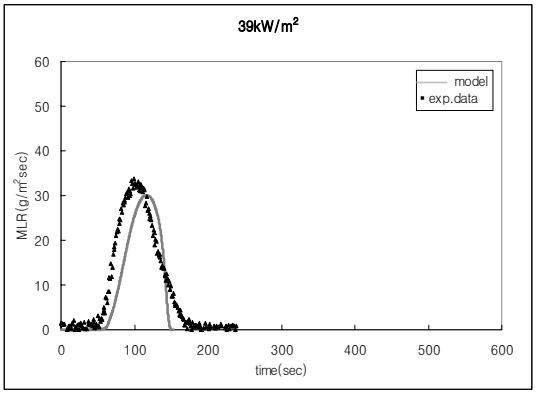

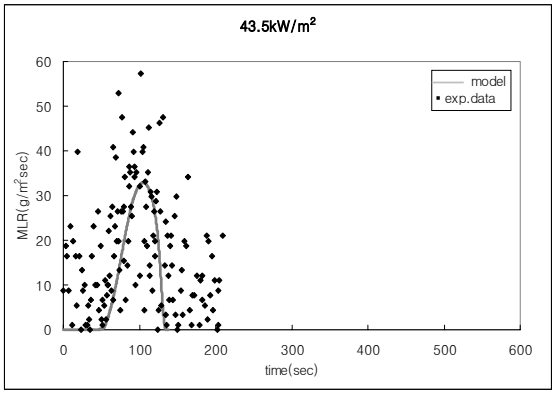

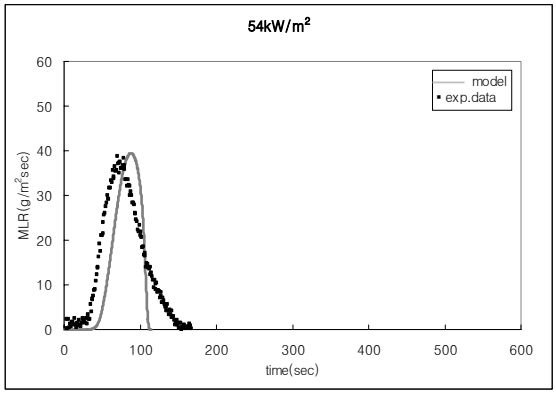
54kW/m²
model
exp.data
MLR(g/m²sec)
time(sec)
0
10
20
30
40
50
60
0
100
200
300
400
500
600

4. Nylon +5% clay with 3.2mm

1) Flaming initiated at the fire point.

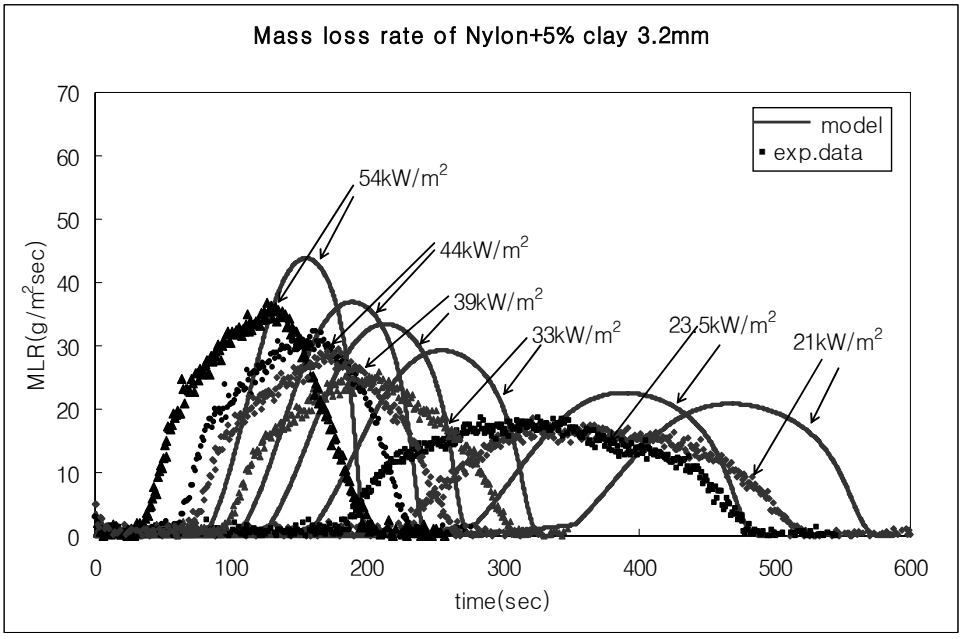

2) Flaming initiated at the flash point.

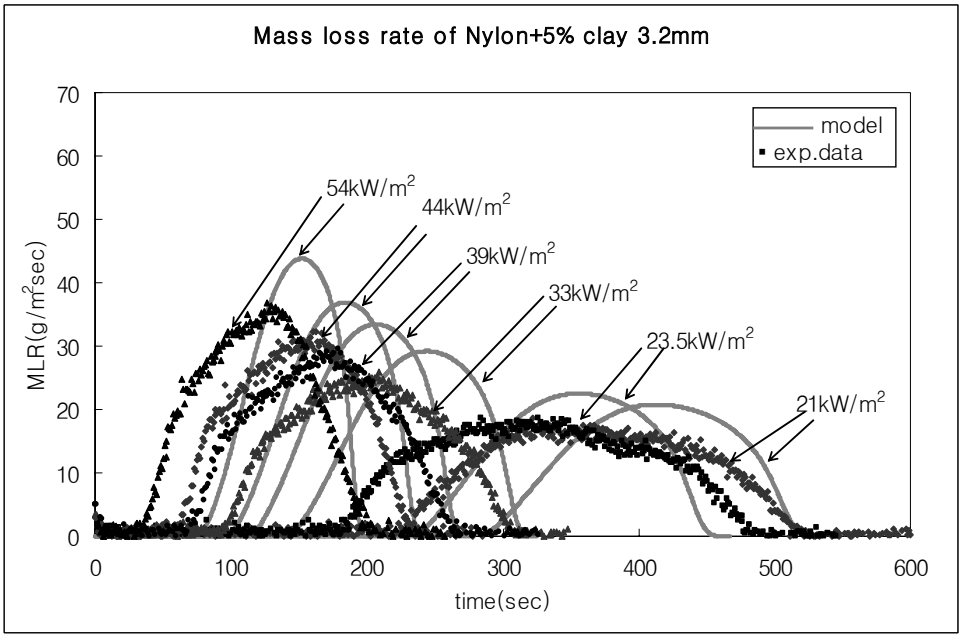

3) Flaming initiated at the flash point.

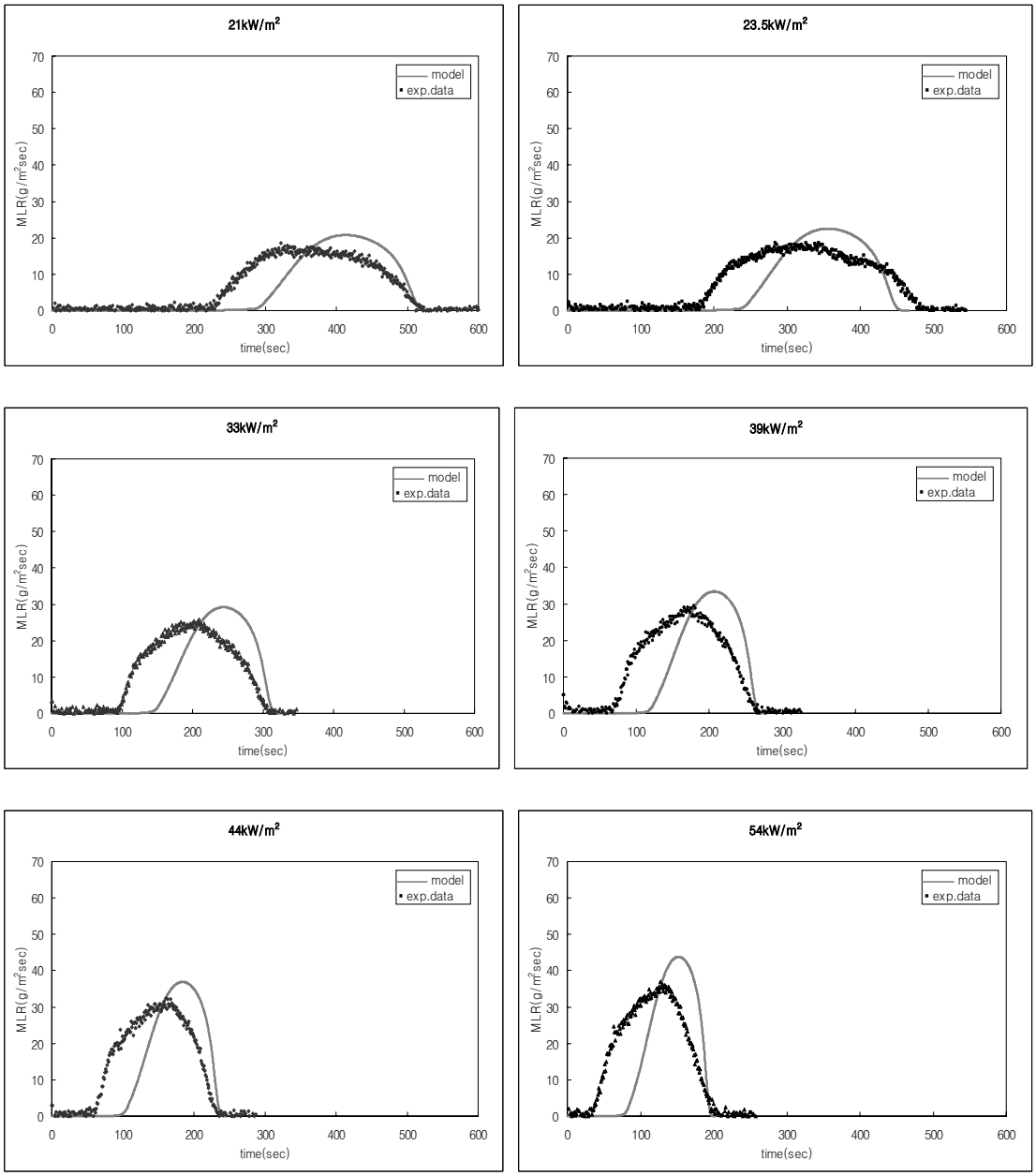

REFERENCE

1. Liu, X., *Flammability properties of clay-nylon nanocomposites*, in *Fire protection engineering*. 2004, University of Maryland.
2. Xin Liu , J.G.Q., *Flammability properties of clay-nylon nano-composites*. December 2004, FAA.
3. Kashiwagi, T., et al., *Flame retardant mechanism of polyamide 6-clay nanocomposites.* Polymer, 2004. **45**: p. 881-891.
4. Rhodes, B.T. and Quintiere, J.G., *Burning rate and flame heat flux for PMMA in a cone calorimeter.* Fire Safety Journal, 1996. **26**: p. 221-240.
5. Jr, D.H. and Quintiere, J.G., *Material fire properties and predictions for thermoplastics.* Fire safety journal, 1996. **26**: p. 241-268.
6. Henderson, J.B., et al., *A method for determination of the specific heat and heat of decomposition of composite materials.* Thermochimica, 1982. **57**: p. 161-171.
7. Ouellette, J. and Lattimer, B.Y., *Properties of composite material for thermal analysis involving fires.*
8. Chris Lautenberger, F.-P., *Pyrolysis modeling, thermal decomposition, and transport process in combustible solids.*
9. Gao, Z., Amasaki, I., and Nakada, M., *A thermogravimetric study on thermal degradation of polyethylene.* Journal of Analytical and Applied Pyrolysis, 2003. **67**: p. 1-9.
10. Kaufmann, E.N., *Characterization of materials*. Vol. 1. 2003: WILEY-INTERSCIENCE.
11. Staggs, J.E.J., *A Theory for Quasi-Steady single-step Thermal Degradationo of Polymers.* Fire and Materials, 1998. **22**(109-118).
12. T.Kashiwagi, R.H.H., X.Zhang, R. M. Briber, B. H. Cipreiano, S. R, Raghavan, W. H. Awad, J. R. Shields, *Flame retardant mechanism of polyamide 6-clay nanocomposite.* Polymer, 2004.
13. Kashiwagi, T., *TGA data for Nylon and Nylon+5% clay with a series of constant heating tares.* 2004.
14. Henderson, J.B., et al., *A method for the determination of the specific heat and heat of decomposition of composite materials.*
15. Ismat A. Abu-Isa, Jodeh, S., and Due, D.L., *Thermal properties of automotive polymers.* 2001: p. 6.
16. Liu, X. and Quintiere, J.G., *Flammability properties of clay-nylon nano-composites*. December 2004, FAA.
17. Quintiere, J.G., *Fundamentals of Fire Phenomena*, ed. 1. 2006.
18. Quintiere, J.G., *A comprehehsive basis for flammability assessment in terms of measurable properties.* 2005.
19. Quintiere, J.G., *A theoretical basis for flammability properties.* Fire and Materials, 2005. **30**: p. 175-214.
20. Jr, D.H. and J.G.Quintiere, *Material fire properties and predictions for thermoplastics.* 1996.

21. Spearpoint, M.J. and J.G.Quintiere, *Predicting the burning of wood using an integral model.* Combustion and Flame, 2000. **123**: p. p.308-324.
22. *Polymer Flammability*, in *dot/faa/ar-05/14*. 2005, FAA.
23. *SFPE handbook*, ed. 3rd. 3-98.